Characterization of a novel separase-interacting protein and candidate new securin, Eip1p, in the fungal pathogen *Candida albicans*

Samantha Sparapani and Catherine Bachewich*
Department of Biology, Concordia University, Montreal, QC H4B 1R6, Canada

ABSTRACT Proper chromosome segregation is crucial for maintaining genomic stability and dependent on separase, a conserved and essential cohesin protease. Securins are key regulators of separases, but remain elusive in many organisms due to sequence divergence. Here, we demonstrate that the separase homologue Esp1p in the ascomycete *Candida albicans*, an important pathogen of humans, is essential for chromosome segregation. However, *C. albicans* lacks a sequence homologue of securins found in model ascomycetes. We sought a functional homologue through identifying Esp1p interacting factors. Affinity purification of Esp1p and mass spectrometry revealed E̲sp1p-I̲nteracting P̲rotein1̲ (Eip1p)/Orf19.955p, an uncharacterized protein specific to *Candida* species. Functional analyses demonstrated that Eip1p is important for chromosome segregation but not essential, and modulated in an APC^{Cdc20}-dependent manner, similar to securins. Eip1p is strongly enriched in response to methyl methanesulfate (MMS) or hydroxyurea (HU) treatment, and its depletion partially suppresses an MMS or HU-induced metaphase block. Further, Eip1p depletion reduces Mcd1p/Scc1p, a cohesin subunit and separase target. Thus, Eip1p may function as a securin. However, other defects in Eip1p-depleted cells suggest additional roles. Overall, the results introduce a candidate new securin, provide an approach for identifying these divergent proteins, reveal a putative anti-fungal therapeutic target, and highlight variations in mitotic regulation in eukaryotes.

INTRODUCTION

Segregation of duplicated chromosomes to two daughter cells during mitosis is essential for maintaining genomic stability. Errors in this process have profound consequences and can lead to numer-

Abbreviations used: ACN, acetonitrile; APC/C, anaphase promoting complex/cyclosome; ARM, armadillo; CDK, cyclin-dependent kinase; DAPI, 4′, 6′-diamidino-2-phenylindole dihydrochloride; DIC, differential interference contrast; Eip1p, E̲sp1p-interacting p̲rotein1̲; FA, formic acid; FEAR, F̲ourteen E̲arly A̲naphase R̲elease; GFP, green fluorescent protein; HU, hydroxyurea; i.d., inside diameter; MEN, mitotic exit network; MMS, methyl methanesulfate; SMC, structural maintenance of chromosome; TAP, tandem affinity purification; TBST, Tris-buffered saline Tween; TEV, tobacco etch virus; YPD, yeast extract peptone.

ous disorders including cancer (Kumar, 2017). During metaphase, sister chromatids align at the equatorial region of the cell and are under tension due to mutual attachment and kinetochore binding to spindle microtubules (Piskadlo and Oliveira, 2017). Chromatids are joined by cohesin, a conserved protein complex (Mehta *et al.*, 2013). In the yeast *Saccharomyces cerevisiae*, this consists of structural maintenance of chromosomes (SMC) proteins Smc1p and Smc3p, the kleisin subunit Mcd1p/Scc1p, and Scc3p. Together these form a ring structure on chromatids after DNA replication (Mehta *et al.*, 2013). To progress to anaphase, cohesin must be cleaved.

Separase is a highly conserved and essential cysteine protease responsible for cleaving Mcd1p/Scc1p and triggering anaphase (Kumar, 2017). In *S. cerevisiae*, absence of the separase homologue *ESP1* results in large-budded cells with unsegregated chromatin, spindle defects, and extra spindle pole bodies (McGrew *et al.*, 1992). In humans, depletion of separase also results in defects in sister chromatid separation (Chestukhin *et al.*, 2003). Cleavage of cohesin by separase is enhanced by phosphorylation of the Mcd1p/Scc1p subunit by polo-like kinases, including PLK-1

in humans or Cdc5p in *S. cerevisiae*, respectively (Alexandru *et al.*, 2001; Hornig *et al.*, 2002; Hauf *et al.*, 2005). Separases have several additional functions (Kumar, 2017). In *S. cerevisiae*, for example, Esp1p is part of the Fourteen Early Anaphase Release or FEAR network where it contributes to initial release of the phosphatase Cdc14p from the nucleolus, which in turn is required for rDNA segregation (Yellman and Roeder, 2015). Cdc14p is released by phosphorylation of the inhibitor Net1p by mitotic cyclin-dependent kinase (CDK) Cdc28p/Clb2p as well as down-regulation of the PP2A^{CDC55} phosphatase by Esp1p and other FEAR components in a nonproteolytic manner (Stegmeier *et al.*, 2002; Sullivan and Uhlmann, 2003). The bulk of Cdc14p is released into the cytoplasm later in mitosis by the mitotic exit network (MEN). This permits Cdc14p-dependent dephosphorylation of several substrates, resulting in down-regulation of mitotic CDK activity and mitotic exit (Weiss 2012). Esp1p also cleaves Slk19p, a kinetochore-associated protein, and both are important for several spindle functions (Havens *et al.*, 2010). Esp1p contributes to mitotic exit through promoting spindle elongation and spindle pole body entry into the bud, a requirement for activation of the MEN pathway (Lu and Cross, 2009; Yellman and Roeder, 2015).

Securin is a critical regulator of separase, and homologues have been characterized in *S. cerevisiae* (Pds1p) (Yamamoto *et al.*, 1996a), *Shizosaccharomyces pombe* (Cut2) (Funabiki *et al.*, 1996), *Homo sapiens* and other mammals (Pttg1) (Zou *et al.*, 1999), *Drosophila melanogaster* (Pim) (Jäger *et al.*, 2001), and *Caenorhabditis elegans* (Ify-1) (Kitagawa *et al.*, 2002). Securin is positively required for separase folding, localization, and stability, but also inhibits enzyme activity (Agarwal and Cohen-Fix, 2002; Hornig *et al.*, 2002; Hellmuth *et al.*, 2015; Luo and Tong, 2018). Securins are initially targeted for degradation at the metaphase-to-anaphase transition to permit rapid activation of separase and abrupt, synchronous chromosome segregation. In *S. cerevisiae*, some securin remains in order to inhibit separase and prevent mitotic exit during anaphase, but is subsequently degraded later in mitosis (Hatano *et al.*, 2016). Degradation is mediated by the anaphase promoting complex/cyclosome (APC/C) and its cofactors Cdc20p and Cdh1p (Kramer *et al.*, 2000; Hilioti *et al.*, 2001; Hatano *et al.*, 2016). In *S. cerevisiae*, *pds1* mutants were initially identified by screening for precocious separation of chromosomes in the presence of microtubule inhibitors (Guacci *et al.*, 1993; Yamamoto *et al.*, 1996a). In the absence of inhibitory drugs, *pds1Δ* cells are viable but show growth defects in the form of heterogeneous and microcolony formation and chromosome loss (Yamamoto *et al.*, 1996a). However, *PDS1* is essential at higher temperature due to a temperature-sensitive defect at G1/S that prevents normal spindle elongation and Esp1p from entering the nucleus, resulting in most cells containing a single DNA mass (Yamamoto *et al.*, 1996a; Jensen *et al.*, 2001). Additional phenotypes include loss of synchrony in separation of sister chromatid pairs, and some multinucleate cells, implying precocious mitotic exit (Holt *et al.*, 2008; Hatano *et al.*, 2016). Securins are essential for growth in *S. pombe*, *D. melanogaster*, and *C. elegans* (Funabiki *et al.*, 1996; Stratmann and Lehner, 1996; Jäger *et al.*, 2001; Kitagawa *et al.*, 2002), but not in vertebrates, due to additional inhibitory regulation of separase by CDK/cyclin B phosphorylation (Hellmuth *et al.*, 2015). Securin becomes essential in *S. cerevisiae* when spindle assembly or kinetochore function is defective, or in response to γ irradiation-induced activation of DNA damage in G2 phase. Under these conditions, it is stabilized through sequestration of Cdc20p by the spindle checkpoint protein Mad2p, or Chk1p-dependent phosphorylation, respectively (Yamamoto *et al.*, 1996a,b; Cohen-Fix

and Koshland, 1997; Wang *et al.*, 2001; Palou *et al.*, 2017). Pds1p is also regulated by CDK/cyclin B phosphorylation, which enhances binding to Esp1p and localization to the nucleus (Agarwal and Cohen-Fix, 2002). Despite the fact that separase, cohesin, and the APC/C are conserved, securins are divergent in sequence and have not been identified in several organisms, including plants and many fungi, for example (Moschou and Bozhkov, 2012).

Candida albicans is a diploid ascomycete that exists in many morphological forms including yeast, pseudohyphal, hyphal, or chlamydospore cells and is one of the most common opportunistic fungal pathogens of humans. A commensal in the gastrointestinal tract, *C. albicans* can also be invasive, causing systemic infections that can be associated with mortality rates reaching 50% (da Silva Dantas *et al.*, 2016). Limited treatments and growing drug resistance (O'Meara *et al.*, 2015) compel identification of new therapeutic targets and anti-fungal therapies, which is dependent on a thorough understanding of the basic biology of the organism (Sellam and Whiteway, 2016).

Cell proliferation is important for survival of *C. albicans* in the host and virulence. However, the cell cycle networks, including those governing chromosome segregation and mitotic progression, are not well defined, and some conserved players show variations in function. For example, several *C. albicans* homologues of MEN factors are required for mitotic exit in a manner similar to the situation in *S. cerevisiae* (Milne *et al.*, 2014; Bates, 2018; Orellana-Muñoz *et al.*, 2018), but others have additional functions (Clemente-Blanco *et al.*, 2006; González-Novo *et al.*, 2009). With respect to the metaphase-to-anaphase transition, *C. albicans* homologues of the APC/C cofactors Cdc20p and Cdh1p are conserved in regulating anaphase onset, telophase, and mitotic exit through targeting the mitotic cyclin Clb2p and the polo kinase Cdc5p for degradation (Chou *et al.*, 2011). However, variations in function were suggested by the pleiotropic phenotype of *cdh1Δ/Δ* cells, which included enlarged yeast-form cells. In contrast, *S. cerevisiae cdh1Δ* cells were significantly reduced in size due to a role for Cdh1p in repressing START (Jorgensen and Tyers, 2004). Further, Cdc20p depletion results in filament formation, contrary to the large doublet arrest of *S. cerevisiae cdc20* mutants (Lim *et al.*, 1998). *C. albicans* has a separase homologue, Esp1p, and its depletion also results in filamentous growth (O'Meara *et al.*, 2015). However, its functions remain unclear. Cohesin homologues are also present, including Mcd1p/Scc1p, but not characterized. Similar to many other fungi, *C. albicans* lacks a sequence homologue of securin. Together with other examples of functional variation in cell cycle regulatory factors (Bachewich *et al.*, 2003; Atir-Lande *et al.*, 2005; Shi *et al.*, 2007; Ofir and Kornitzer, 2010; Ofir *et al.*, 2012; Mendelsohn *et al.*, 2017) and cell cycle phase expression of *C. albicans*-specific genes (Cote *et al.*, 2009), the data imply unique facets of the cell cycle circuitry in *C. albicans*, which could be exploited for the purpose of controlling growth. *C. albicans* is tolerant of aneuploidy and exploits this feature as a mechanism for adapting to different environments (Selmecki *et al.*, 2010), further underscoring the need to understand the mechanisms governing chromosome segregation in this organism.

To gain new insights on the regulation of the metaphase-to-anaphase transition and mitotic progression in *C. albicans*, we characterized the separase homologue Esp1p and demonstrate that it is essential for sister chromatid segregation. Further, we identified a novel Esp1p-binding protein, Esp1p-Interacting Protein1 (Eip1p). Eip1p is *Candida*-specific, important for chromosome segregation, and has other features consistent with it being a candidate securin with possible additional functions.

RESULTS

Depletion of Esp1p results in growth inhibition, bud enlargement, and filamentation

We previously characterized the *C. albicans* APC/C cofactor Cdc20p and demonstrated that it is important for the metaphase-to-anaphase transition (Chou *et al.*, 2011). However, its precise mechanisms of action remain unclear. Securins are targets of Cdc20p, but highly divergent in sequence (Bachmann *et al.*, 2016). *C. albicans* lacks a sequence homologue of the few known securins in other ascomycetes. We hypothesized that a functional homologue may be revealed by identifying factors that copurify with a protein that is known to bind securin. Since the interaction between Cdc20p and securin is transient (Hilioti *et al.*, 2001), we focused on another conserved securin partner, separase. *C. albicans* contains a separase homologue, *ESP1/ORF19.3356* (www.candidagenome.org). Esp1p is similar to other separases with respect to the catalytic domain, armadillo (ARM) repeats and regions of disorder (Figure 1A) and is 23.2% identical and 40.5% similar to Esp1p from *S. cerevisiae*. A screen of *C. albicans* strains under control of the *TET* promoter demonstrated that *ESP1* is essential, and its repression results in filamentous growth (O'Meara *et al.*, 2015). However, the functions of Esp1p, including a role in mitosis, remain unclear. We first addressed this question by creating a strain carrying a single copy of *ESP1* under control of the *MET3* promoter. When plated on solid repressing medium at 30°C for 24 h, the strain grew poorly and was filamentous. In contrast, normal growth was observed for wild-type cells on repressing medium, or both strains on inducing medium (Figure 1B). In liquid-repressing medium, cells lacking Esp1p were predominantly large-budded by 5 h and filamentous by 24 h. In contrast, normal yeast-form cells were observed under inducing conditions and in the control strain in both media (Figure 1C; Table 1). Similar results were obtained when we repressed *ESP1* with the *TET* promoter using doxycycline (Supplemental Figure S1), in agreement with previous results (O'Meara *et al.* 2015). In comparison, *S. cerevisiae* cells lacking Esp1p arrest as large doublets (Baum *et al.*, 1988). Thus, the absence of Esp1p in *C. albicans* impairs yeast cell division, resulting in bud enlargement and filamentation.

Depletion of Esp1p prevents chromosome segregation and impairs spindle elongation

In *S. cerevisiae*, the absence of functional Esp1p prevents chromosome segregation and proper spindle formation (McGrew *et al.*, 1992). To determine whether *C. albicans* Esp1p has similar functions, the conditional *ESP1* and control strains were incubated in inducing or repressing medium for 8 h, fixed, and stained with 4′,6′-diamidino-2-phenylindole dihydrochloride (DAPI). In repressing medium, ~ 55% of cells depleted of Esp1p contained enlarged buds with a single mass of DNA near or within the bud neck. In contrast, this was observed in ~ 20% of cells under inducing conditions, or in wild-type cells in both media (Figure 2; Table 1). Similar results were obtained when *ESP1* was repressed with doxycycline in a strain carrying a single copy of *ESP1* under control of the *TET* promoter (Supplemental Figure S1B). This localization reflects metaphase/early anaphase (Hazan *et al.*, 2002) or movement of a preanaphase nucleus into the bud, which is associated with many conditions that arrest early mitosis in *C. albicans* (Bai *et al.*, 2002; Bachewich *et al.*, 2003, 2005; Bensen *et al.*, 2005). Thus, Esp1p is important for chromosome segregation in *C. albicans*, consistent with it functioning as a separase.

Esp1p in *S. cerevisiae* is also important for spindle formation and elongation (Jensen *et al.*, 2001). To determine whether *C. albicans* Esp1p influences spindle organization, β-tubulin was tagged with GFP (Hazan *et al.*, 2002; Finley and Berman, 2005) in the *MET3::ESP1* conditional strain. After incubating in inducing medium for 7 h, 7.0% (*n* = 186) of cells contained short rod-like spindles characteristic of metaphase or early anaphase, while 8.1% contained elongated late anaphase spindles that spanned the mother and daughter cells (Figure 2). The remaining cells contained a spot of Tub2p-GFP signal, representing a spindle pole body in G1 phase, or an enlarged spot corresponding to a duplicated spindle pole body in S/G2 phase (Hazan *et al.*, 2002). In repressing medium, 45.3% (*n* = 148) of cells contained short rod spindles (Figure 2), and elongated late anaphase spindles were not observed. The remaining cells demonstrated a spindle pole body, at times more than one, cytoplasmic microtubules or abnormal microtubule organization. Notably, the Tub2p-GFP-tagged strain showed transient filamentation when transferred from overnight to fresh medium, irrespective of composition. However, by 7 h, the majority of cells in inducing medium were in a yeast form, while those in repressing medium resembled the phenotype of the untagged conditional strain. The results suggest that Esp1p is important for spindle elongation.

Identification of Esp1p-interacting factors reveals strong enrichment of an uncharacterized protein, Eip1p/Orf19.955p

If Esp1p is a separase, we reasoned that one of its interacting proteins may be a functional homologue of a securin. To test this hypothesis, strains carrying a single copy of *ESP1* tagged at the C-terminus with the tandem affinity purification (TAP) tag composed of protein A and calmodulin-binding peptide, separated by a tobacco etch virus (TEV) protease cleavage site (Lavoie *et al.*, 2008), were created. Since cells expressed the protein and grew at normal rates (unpublished data), Esp1p-TAP was deemed functional. Affinity purification of Esp1p-TAP was performed in exponential-phase cells, but copurifying proteins were not greatly enriched (unpublished data). We thus tagged *ESP1* with TAP in a *CDC20* conditional strain to allow for a synchronized block in mitosis and potential enhancement of interacting proteins. Cells from the TAP-tagged and an untagged control strain were incubated in inducing medium overnight, diluted into repressing medium, incubated for 4 h prior to collection, and processed for LTQ-Orbitrap Elite with nano-ES analysis. After removal of peptides that were also present in the untagged strain, the data revealed strong enrichment of Esp1p, the phosphatase Cdc14p, and Orf19.955p, a previously uncharacterized protein with no close sequence homologues (Figure 3A; Supplemental Table S4). Additional copurifying peptides corresponded to proteins of varying function, including the heat shock protein *HSP70*, the filamentation regulator *DEF1*, and the endocytosis-associated protein *CTA3*, for example. Notably, homologues of proteins that interact with Esp1p in *S. cerevisiae*, including the protein kinase Cdc5p (Rahal and Amon, 2008), the protein phosphatase regulatory subunit Cdc55p (Queralt and Uhlmann, 2008), the cohesin complex protein Mcd1p/Scc1p (Uhlmann *et al.*, 2000), and the kinetochore-associated protein Slk19p (Rahal and Amon, 2008) did not coprecipitate with *C. albicans* Esp1p. A previous report of phenotypes of *TET*-regulated strains of *C. albicans* indicated *ORF19.955* was essential and influenced filamentous growth (O'Meara *et al.*, 2015), but its precise functions remain unclear. Since Orf19.955p was one of the most enriched Esp1p-interacting proteins and of novel sequence, we hypothesized that it may be a candidate functional securin. The remainder of the study focused on this protein, Esp1p-Interacting Protein1 (Eip1p).
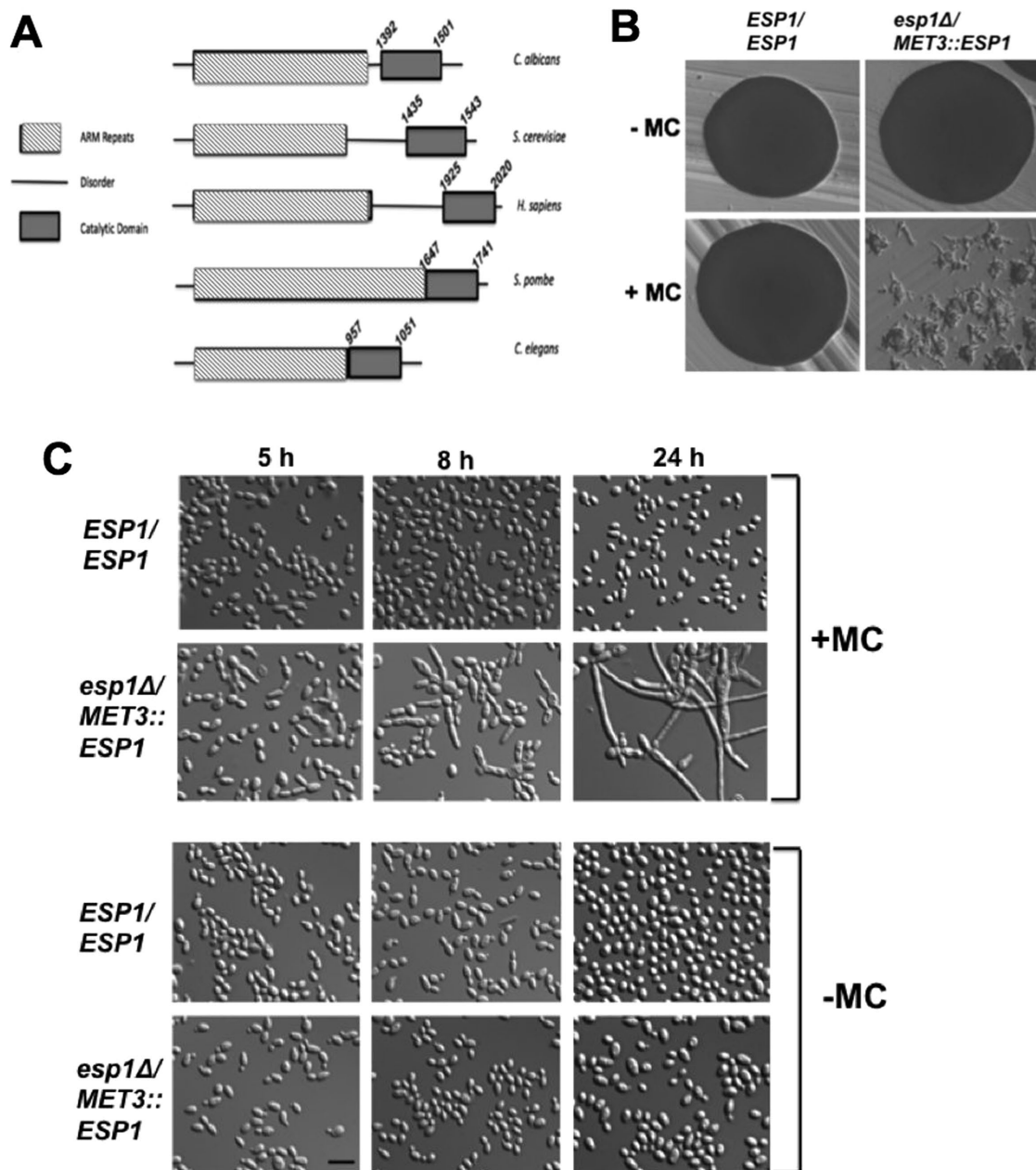
FIGURE 1: *C. albicans* Esp1p is conserved in sequence and its depletion results in large bud formation, filamentation, and growth inhibition. (A) Comparative analysis of amino acid sequences of separase homologues from *C. albicans* (Esp1p), *S. cerevisiae* (Esp1p), *H. sapiens* (ESPL1), *S. pombe* (Cut1), and *C. elegans* (Sep-1). Amino acid sequences were obtained from the *Saccharomyces* Genome Database (www.yeastgenome.org), *Candida* Genome Database (www.candidagenome.org), WormBase (www.wormbase.org/#012-34-5), Pombase (www.pombase.org), and UniProt (www.uniprot.org), respectively. Sequences were analyzed with InterPro (www.ebi.ac.uk/interpro/) and information in Bachmann *et al.* (2016). (B) Strains BH440 (*ESP1/ESP1*, *URA+HIS+*) and SS35 (*esp1::URA3/MET3::ESP1-HIS1*) were streaked onto solid repressing (+MC) or inducing (–MC) medium and incubated at 30°C for 24 h. (C) Overnight cultures of strains BH440 or SS35 were diluted into liquid –MC or +MC medium and incubated at 30°C for the indicated time periods. Bar: 10 µm.

To confirm that Eip1p and Esp1p physically interact, we performed coimmunoprecipitation. For this purpose, strains containing *EIP1* tagged at the C-terminus with the MYC epitope alone or in combination with *ESP1* tagged with the HA epitope were constructed. Immunoprecipitation of Esp1p-HA with anti-HA beads copurified Eip1p-MYC (Figure 3B; full blot in Supplemental Figure S2). Eip1p-MYC did not copurify from cells with untagged Esp1p. Thus, Esp1p and Eip1p physically interact.

Eip1p is a novel, *Candida*-specific protein that contains putative KEN and destruction boxes

EIP1 encodes a potential protein of 325 amino acids and a predicted molecular weight of 36.4 kDa (www.candidagenome.org). A BLAST search of the *EIP1* sequence against all known organisms (http://blast.ncbi.nlm.nih.gov/Blast.cgi) or against fungi alone (www.yeastgenome.org) revealed that the only homologues were in several *Candida* species (Supplemental Figure S3). Securins

+MC							
esp1Δ/MET3::ESP1 (n = 155)	19.3	22.4	22.4	6.2	4.3	15.5	9.9
ESP1/ESP1 (n = 161)	63.0	15.5	0	5.2	0	1.0	15.4
–MC							
esp1Δ/MET3::ESP1 (n = 269)	70.9	12.0	0	2.6	0	0	14.5
ESP1/ESP1 (n = 253)	54.0	24.0	0	3.1	0	0	19.4

The percentage of cells showing the indicated patterns. Strains SS35 (*esp1::URA3/MET3::ESP1-HIS1*) and BWP17 (*ESP1/ESP1*) were incubated in –MC or +MC medium for 8 h, fixed, and stained with DAPI.

TABLE 1: Number and distribution of nuclei in Esp1p-depleted cells.

are not well conserved at the sequence level (Bachmann *et al.*, 2016) and consistently, an alignment of Eip1p with securins PTTG1, Pds1p or Cut2 showed little similarity (Supplemental Figure S4). However, Eip1p has some features consistent with securins. It contains putative destruction boxes (Cohen-Fix *et al.*, 1996) and a KEN box (Yamamoto *et al.*, 1996a) (Figure 3C). Eip1p also contains one consensus phosphorylation site for CDK, similar to PTTG1 (Ramos-Morales *et al.*, 2000), and numerous sites for polo-like kinase phosphorylation (Figure 3C). In contrast, Pds1p contains five phosphorylation sites for CDK (Agarwal and Cohen Fix, 2002). To explore the *EIP1* sequence further, a 3D structure analysis comparison using the program Phyre2 Protein Folder was performed. Intriguingly, the results demonstrated 50% confidence, in alignment at a specific region with Pds1p, and some similarity in the predicted 3D structure based on this alignment (Figure 3D). Thus, Eip1p is a *Candida*-specific protein but has some features consistent with other securins.

esp1Δ/MET3::ESP1, TUB2/TUB2-GFP

FIGURE 2: Depletion of Esp1p impairs chromatin separation. Strain SS37 (*TUB2-GFP-ARG4/TUB2, esp1::URA3/MET3::ESP1-HIS1*) was incubated in inducing (–MC) or repressing (+MC) medium for 7 h, mounted, and imaged live. An arrowhead denotes a G2-M/early anaphase spindle. The arrow indicates a late anaphase spindle. The star denotes two spindle pole bodies within one cell. Bar: 10 μm.

Depletion of Eip1p impairs cell growth and morphology

To address the function of Eip1p, we created a conditional strain containing a single copy of the gene under control of the *MET3* promoter. When plated on solid repressing medium at 30°C for 24 h, growth was severely restricted. Only a few small colonies formed, in contrast to the situation with wild-type cells or when both strains were plated on inducing medium (Figure 4A). To explore the growth defect further, serial dilutions of strains were spotted onto plates and incubated for 24, 48, or 72 h. The *ESP1* conditional strain was included for comparison. By 72 h, growth of the *EIP1* conditional strain remained impaired relative to wild-type cells on repressing medium (Figure 4B). However, a low level of colony growth was observed. Intriguingly, this was variably more than that of Esp1p-depleted cells. With the *TET*-regulated strains, Eip1p-versus Esp1p-depleted cells consistently demonstrated some residual growth (8/8 trials) (Supplemental Figure S5, A and B). This result prompted an attempt to create a strain lacking both alleles of *EIP1* (*eip1::URA3/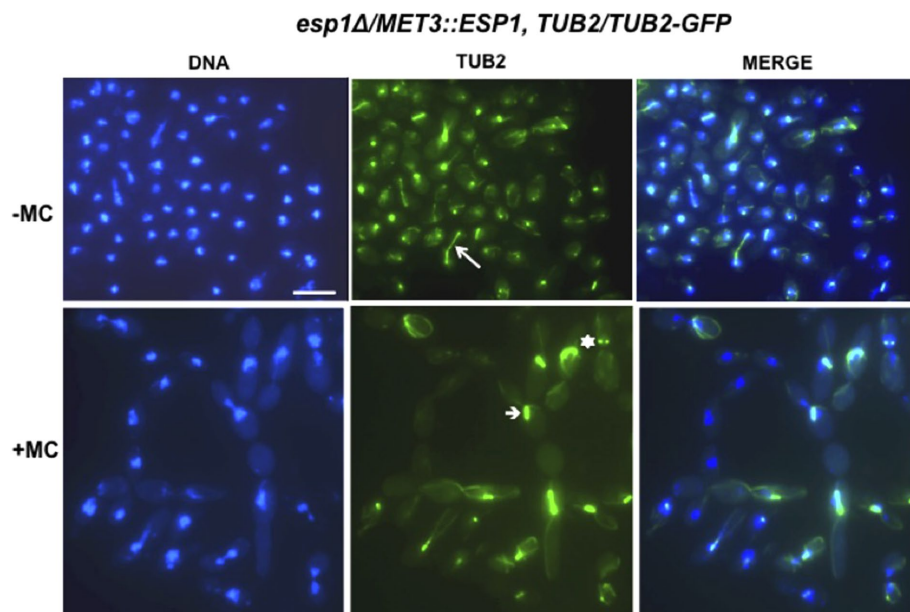eip1::HIS1*). From three separate transformations yielding 23 total transformants, three were positive for replacement of *EIP1* alleles with *HIS1* and *URA3* markers and absence of *EIP1* (Supplemental Figure S6A). The strains grew very slowly (Supplemental Figure S6B) and resembled Eip1p-depleted cells (Supplemental Figure S6C). We cannot rule out the possibility of secondary mutations or chromosomal alterations that permit growth in *eip1Δ/Δ* strains, but it is noteworthy that the strains were recovered from independent transformations. Weak growth could reflect variable accumulations of abnormal events that eventually prevent proliferation. In comparison, securins from *S. pombe* and *D. melanogaster*, for example, are essential (Funabiki *et al.*,1996, Jager *et al.*, 2001), as well as *PDS1* of *S. cerevisiae* at 37°C, where cells arrest in a large-budded form due to a temperature-sensitive defect at the G1/S transition that affects spindle elongation and Esp1p localization into the nucleus (Yamamoto *et al.*, 1996a; Jensen *et al.*, 2001; Agarwal and Cohen-Fix, 2002). At lower temperature, however, *pds1Δ* cells are viable but chromosome loss is frequent and many cells cannot form colonies

A Orbitrap LC/MS analysis of putative Esp1p-interacting proteins

PROTEIN ID	Peptides	ORF	Identified Proteins
CAL0004160	63	ESP1	Putative caspase-like cysteine protease;
CAL0005886	24	CDC14	Protein involved in exit from mitosis and morphogenesis
CAL0003715	11	ORF19.955	UNCHARACTERIZED, protein of unknown function
CAL0000006	8	HSP70	Putative hsp70 chaperone;
CAL0005977	6	CDC19	Pyruvate kinase at yeast cell surface; Gcn4/Hog1/GlcNAc regulated;
CAL0000121	4	DEF1	RNA polymerase II regulator; role in filamentation, epithelial cell escape

B

ANTI-HA

ANTI-MYC

C Eip1p (325 aa)

MSSHIFKDIQ DKENELKTSG IRRKGIISNE NAGPLLSKDS NSRQVQQPQQ
TQQQQQQSKF TNKRIPLGGK NHNSNKLLLN RSQSSLNTKP TTQGITNVKP
PSLPKSNSSL GFSVVSDQPT EQQKQLPQPFVVHNEQVLPVKRKLLQDTKD
ELSQNSKRVK LEKKESNANT FTDSLTKPTQ NVLAHVDDLQ TTISSKTDQL
NSSNLTHNDI NRNNVDPVKR NSRLKAIDDL VESHWQDPIE TIPETVGAEN
NNGEQLEELD IKFFSTPNES FDIGDLDENH LANNEQKLSL ELDFEDESNV
GEIPIIEGID EEIGLTSDDL DNLLG

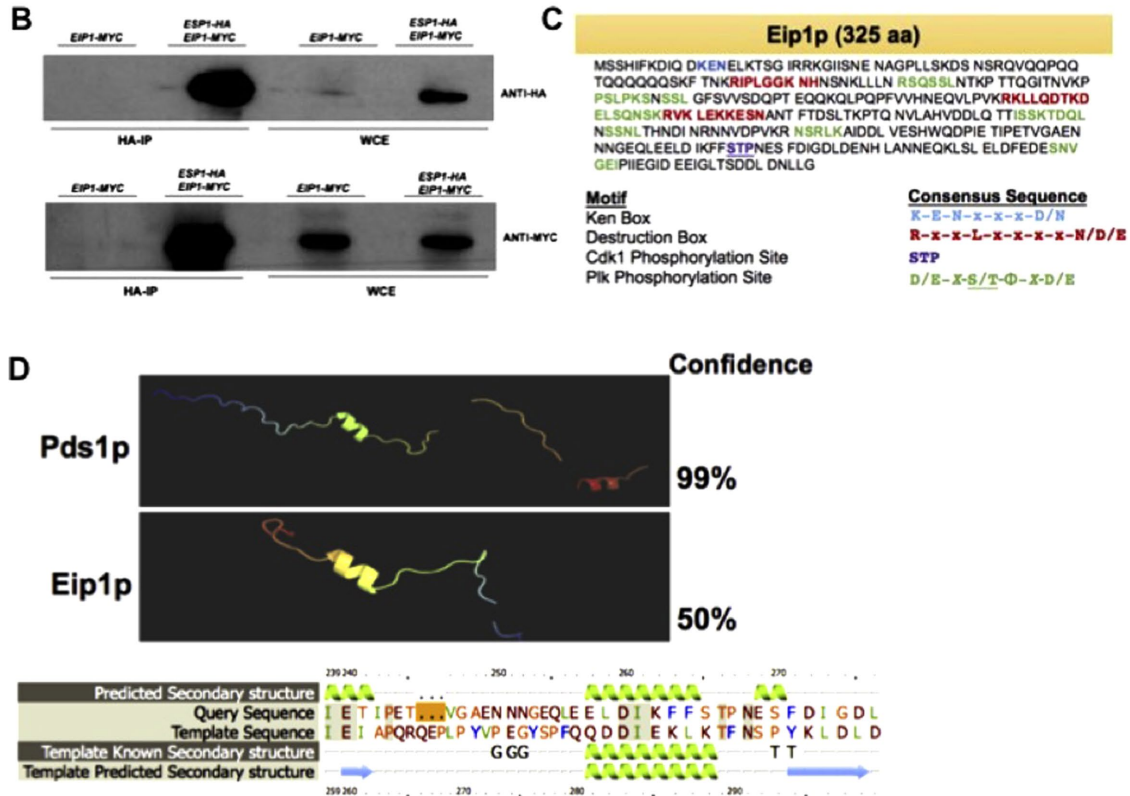| Motif	Consensus Sequence
Ken Box	K-E-N-x-x-x-D/N
Destruction Box	R-x-x-L-x-x-x-x-N/D/E
Cdk1 Phosphorylation Site	STP
Plk Phosphorylation Site	D/E-x-S/T-Φ-x-D/E

D

Pds1p — Confidence 99%

Eip1p — 50%

FIGURE 3: Identification of Esp1p-interacting proteins reveals Eip1p/Orf19.955p. (A) Select interacting factors of Esp1p-TAP identified by Orbitrap LC/MS analysis. (B) Coimmunoprecipitation confirms a physical interaction between Esp1p and Eip1p. Western blots of whole cell extracts (WCE) and immune-precipitates (HA-IP) of strains SS22 (eip1::URA3/EIP1-MYC-HIS1, ESP1/ESP1) and SS29 (EIP1/EIP1-MYC-HIS1, ESP1/ESP1-HA-URA3) using anti-HA agarose (HA-IP). Blots were incubated with anti-MYC or anti-HA antibody. (C) Eip1p amino acid sequence (Candida Genome Data base; www.candidagenome.org), with motifs indicated. (D) 3D protein simulation using PHYRE 2.0 demonstrating some similarity at a specific region with Pds1p from S. cerevisiae. Bottom portion represents the region of amino acid sequence homology between the template strain (Pds1p) and query strain (Eip1p). Green coils and blue arrows represent regions of α-helices and β-pleaded sheet arrangements, respectively. Polar properties of the protein sequences are shown in colored amino acids. Secondary structures are represented by the number of "G" and "T" segments present, where G indicates a 3-turn α-helix and T represents a hydrogen-bonded turn.

(Yamamoto et al., 1996a; Liang et al., 2013). Eip1p-depleted cells did not show any temperature sensitivity (unpublished data) and the defects were more severe than those of pds1Δ cells at permissive temperature. To determine the dynamics of Eip1p depletion on cell viability, the proportions of cells that stained with propidium iodide during a time course were determined. After 5, 8, or 24 h in repressing medium, 11.3% (n = 194), 9.5% (n = 158), or 30.0% (n = 166) of Eip1p-depleted cells stained with propidium iodide compared with 2.9% (n = 171), 1.3% (n = 157), or 1.5% (n = 198) of cells in inducing medium. Many more Eip1p-depleted cells were clearly inviable at 24 h but lacked cytoplasm, which precluded staining (Supplemental

Figure S7). Thus, Eip1p is critical for growth, but its absence does not immediately lead to death for all cells.

To investigate the phenotype of cells lacking Eip1p, the EIP1-conditional and control strains were incubated in liquid medium at 30°C for set times. After 5 h in repressing medium, Eip1p-depleted cells were in various stages of yeast cell budding (Figure 4C). By 8 h, a pleiotropic phenotype was observed, including enlarged single yeast cells, chains of yeast, or pseudohyphae (Figure 4C; Table 2). When Eip1p was depleted using the TET promoter, similar results were obtained (Supplemental Figure S5C). The results suggest that Eip1p is also important for proper yeast cell morphology.
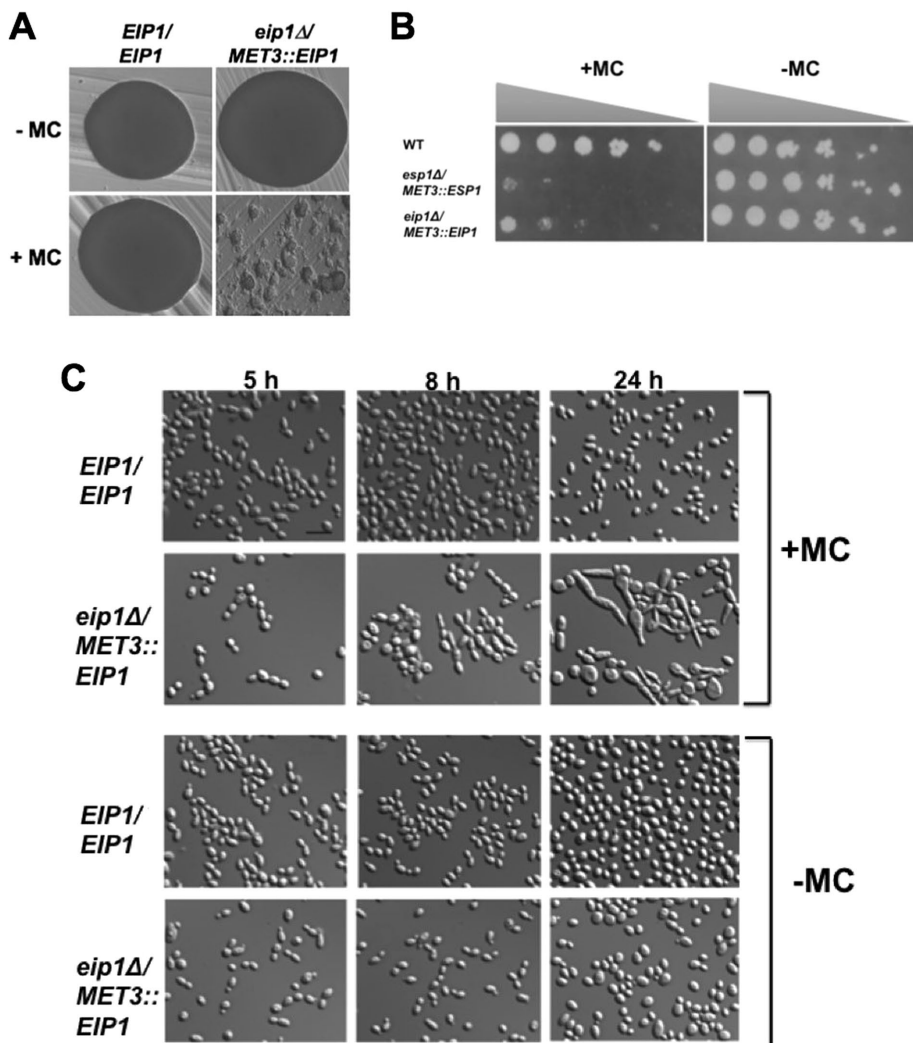
FIGURE 4: Depletion of Eip1p in yeast impairs growth and results in a pleiotropic phenotype including cell enlargement and formation of chains of cells and pseudohyphae. (A) Strains BH440 (*EIP1/EIP1*, *URA3*+*HIS1*+) and SS25 (*eip1::URA3/MET3::EIP1-HIS1*) were streaked onto repressing (+MC) or inducing (–MC) solid medium and incubated at 30°C for 24 h. (B) Strains SS25, BH440, and SS35 (*esp1::URA3/MET3::ESP1-HIS1*) serial diluted onto solid inducing or repressing medium and incubated for 72 h at 30°C. (C) Overnight culture strains BH440 and SS25 were incubated at 30°C, diluted into inducing (–MC) or repressing (+MC) medium, and incubated for the indicated time periods. Bar: 10 μm.

Absence of *EIP1* influences chromosome organization

Absence of essential securins, such as cut2, prevents chromosome segregation and phenocopies separase mutants due to the positive and negative effects of securin on separase (Funabiki *et al.*, 1996; Hellmuth *et al.*, 2015). In contrast, chromosomes segregate successfully and initiate anaphase in a timely manner in the absence of *S. cerevisiae* Pds1p at lower temperature, since it is not essential under these conditions. However, an increase in chromosome loss was noted (Yamamoto *et al.*, 1996a; Alexandru *et al.*, 1999; Liang *et al.*, 2013). At restrictive temperature when *PDS1* is essential, the majority of *pds1Δ* cells are large-budded with an unseparated mass of DNA. Spindles cannot elongate properly, the synchrony of chromatid pair separation is reduced, and some cells are multinucleate, suggesting precocious mitotic exit (Yamamoto *et al.*, 1996a; Ciosk *et al.*, 1998; Holt *et al.*, 2008; Hatano *et al.*, 2016). To determine whether Eip1p influences chromosome segregation, the *EIP1* condi-

tional and wild-type strains were incubated in inducing or repressing medium for 8 h, fixed, and stained with DAPI. Under inducing conditions, the *EIP1*-conditional strain demonstrated normal DNA patterns including single compacted masses per cell compartment, a stretched organization within the bud neck indicative of anaphase, or two separate DNA masses at opposite poles of mother and daughter cells, reflecting late anaphase and/or mitotic exit. Similar patterns were observed in wild-type cells under inducing and repressing conditions (Figure 5A). In contrast, Eip1p-depleted cells demonstrated numerous defects, including irregular-shaped, enlarged DNA masses, more than one DNA mass per cell compartment, and either small fragments or no DNA in some other cells (Figure 5A; Table 2). Further, more cells showed an anaphase-like organization of chromosomes, where DNA was localized within the bud neck, suggesting a delay in mitosis (Table 2). Notably, most cells contained DNA, indicating that chromosome segregation was not homogeneously inhibited. Similar defects were detected when Eip1p was depleted using the *TET* promoter (Supplemental Figure S5C), when both alleles were deleted (Supplemental Figure S6C) or in Eip1p-depleted cells at 37°C (unpublished data).

To investigate the effects of depleting Eip1p on chromosome segregation in living cells, histone *HTB1* was tagged with green fluorescent protein (GFP) (Sherwood and Bennett, 2008) in the *EIP1*-conditional strain. Cells were incubated in inducing or repressing medium for 8 h, and analyzed live with microscopy. Under inducing conditions, cells showed normal DNA patterns as described for DAPI-stained cells. However, in repressing medium, pleiotropic effects were observed, including large irregular-shaped masses of DNA, cells containing two DNA masses, or cells with fragments or no detectable DNA (Figure 5, B and C), similar to fixed cells stained with DAPI. We next performed time-lapse microscopy to analyze the dynamics of chromosome segregation. Cells incubated in inducing medium were transferred to either fresh inducing or repressing medium for 5 h, mounted on an eight-well μSlide, and recorded for 3 h, with images captured every 5 min. In inducing medium, a representative unbudded cell with a single mass of Htb1p-GFP signal demonstrated bud formation followed by anaphase, represented by DNA stretching through the bud neck by 75 min. This was followed by complete separation of signal between mother and daughter cell by 90 min (Figure 5Da; Supplemental Movie S1). In repressing medium, a representative large-budded cell with a large mass of DNA within one compartment did not demonstrate any segregation during the length of the time course (Figure 5Db), while another cell demonstrated uneven separation of Htb1p-GFP signal within the mother cell (Figure 5Dc; Supplemental Movie S2). In another example, an unbudded cell within a cell group

						a	b	c
+MC								
eip1Δ/MET3::EIP1 (n = 242)	51.2	14.5	11.6	3.7	19.0	20.7	5.0	18.2
EIP1/EIP1 (n = 279)	77.4	11.1	1.8	9.7	0	12.5	0	5.7
−MC								
eip1Δ/MET3::EIP1 (n = 269)	75.1	17.5	1.9	5.2	0	5.2	0	7.4
EIP1/EIP1 (n = 253)	85.4	5.5	4.7	4.3	0	12.6	0	2.4

The percentage of cells showing the indicated patterns. Strains BH440 (*EIP1/EIP1, URA3+HIS1*+) and SS25 (*eip1::URA3/MET3::EIP1-HIS1*) were incubated in +MC or −MC medium for 8 h, fixed, and stained with DAPI.
[a]Proportion of total cells lacking visible DAPI staining.
[b]Proportion of total cells containing more than one DAPI-staining body.
[c]Proportion of total cells with abnormal DAPI-stained organization.

TABLE 2: Number and distribution of nuclei in Eip1p-depleted cells.

demonstrated a stretching of Htb1p-GFP signal and separation into two masses within 60 min and remained separated for the duration of the time course (Figure 5Dd, arrow). Within a separate cell group, a small-budded cell demonstrated stretching of the Htb1p-GFP signal by 45 min within the mother cell (Figure 5De, bottom arrow; Supplemental Movie S3). This was oriented perpendicular to the mother/bud axis, but subsequently rearranged parallel to the axis and separated into two masses, one of which entered the small bud 120 min following the initial stretching of Htb1p-GFP signal. Within this same group, a budded cell demonstrated anaphase by 30 min and chromosome segregation between mother and bud (Figure 5De, top arrow). However, 60 min after anaphase, the single Htb1p-GFP mass within the mother cell migrated into the bud, then translocated back to the mother cell 15 min later. A different cell within this group appeared to lack Htb1p-GFP signal (Figure 5De, bottom cell) and imploded 90 min into the time course. Thus, Eip1p-depleted cells can segregate chromosomes, but variably show multiple defects as well as abnormal nuclear movements, suggesting a role for Eip1p in these processes.

Absence of *EIP1* affects spindle orientation and disassembly
Since defects in chromosome segregation can reflect deregulated spindle function, we next analyzed microtubules by tagging β-tubulin with GFP in the Eip1p-conditional strain. Cells were incubated in either inducing or repressing medium and imaged live (Figure 6A) or fixed and stained with DAPI (Figure 6, B and C). In inducing medium, 15.9% and 3.4% (n = 387) of cells showed short bar-like spindles, characteristic of metaphase/early anaphase, or elongated late anaphase spindles that spanned mother and daughter cells, respectively. The remaining cells contained spindle pole bodies (Figure 6A). In repressing medium, however, ~ 45% (n = 309) of Eip1p-depleted cells contained mitotic spindles, where 29.4% were short bars and 14.6% were elongated (Figure 6, A–C). Some spindles appeared normal while others were abnormal in shape or misoriented with respect to the mother/bud axis. Abnormal microtubule structures were also observed (Figure 6, A and B). Some Eip1p-depleted cells also contained single DNA masses with more than one spindle pole body or short spindle, or demonstrated uneven chromosome segregation (Figure 6, B and C). To investigate spindle dynamics, time-lapse imaging of Tub2p-GFP was performed, as described for Htb1p-GFP. Under inducing conditions,

the length of time that cells maintained a short bar spindle, indicative of metaphase or early anaphase, was 9.1 ± 0.8 min (n = 17; SEM), while elongated late anaphase spindles were maintained for 7.9 ± 0.8 min (n = 17; SEM) (Figure 6Da; Supplemental Movie S4). The timing is approximate due to the 5-min intervals for image capture. In contrast, a sample of cells under repressing conditions maintained early anaphase spindles for 98.3 ± 16 min (n = 15; SEM), or elongated late anaphase spindles for 59.2 ± 16.6 min (n = 12; SEM). Variation within these groups was great, however, with some cells maintaining spindles for the duration of the time course (Figure 6Db; Supplemental Movie S5) and others demonstrating normal timing. We also noted random and severe oscillations of some spindles or spindle pole bodies at times back and forth between the mother cell and buds, as described for Htb1p-GFP (Figure 6D, b and c; Supplemental Movies S5 and S6). In comparison, *pds1Δ* cells of *S. cerevisiae* at permissive temperature can form spindles and have normal cell cycle progression (Yamamoto *et al.*, 1996a). At restrictive temperature, spindles frequently fail to elongate or retract back to shorter structures (Yamamoto *et al.*, 1996a; Holt *et al.*, 2008) due to the temperature-sensitive step at G1/S that requires Pds1p for localizing Esp1p to the nucleus and spindle elongation (Jensen *et al.*, 2001; Agarwal and Cohen Fix, 2002). Excess spindle pole bodies are also present since cells do not arrest the cell cycle. However, if *pds1Δ* cells are shifted to 37°C after S phase, spindles can elongate (Yamamoto *et al.*, 1996a). Thus, Eip1p is not essential for spindle formation, but its absence can influence spindle behavior and organization.

Eip1p is significantly reduced when cells are blocked in mitosis through depletion of Cdc5p, but not Cdc20p
Securins are regulated in part through APC/C-dependent degradation. In *S. cerevisiae*, for example, the securin Pds1p is targeted for degradation at the metaphase-to-anaphase transition by the APC/C in association with its cofactor Cdc20p (Cohen-Fix *et al.*, 1996; Funabiki *et al.*, 1996). Residual Pds1p is subsequently targeted by Cdh1p-dependent APC/C activity to permit mitotic exit (Hatano *et al.*, 2016). Pds1p is thus unstable and significantly reduced in late stages of mitosis or G1 phase. Although the APC/C has not been extensively investigated in *C. albicans*, cofactors Cdc20p and Cdh1p were demonstrated to be important for mitotic progression. Depletion of Cdc20p initially resulted in an early mitotic arrest, but most

cells subsequently progressed to late mitosis with two separate DNA masses and elongated spindles (Figure 7B) (Chou et al., 2011). If Eip1p acts as a securin, it may demonstrate APC/C-dependent modulation in mitosis. To test this hypothesis, Eip1p was tagged with the TAP epitope in a *CDC20*-conditional strain (Chou et al., 2011). This and a wild-type strain carrying a TAP-tagged copy of Eip1p were incubated in inducing or repressing medium for set times and processed for Western blotting. In repressing medium, Eip1p was induced in half of the trials ($n = 4$) at 3 h and two-thirds of the trials ($n = 3$) at 6 h, with levels ranging from 1.3 to 1.7 times that of Eip1p-TAP in the control strain (Figure 7A). In inducing medium where cells overexpressed *CDC20*, Eip1p-TAP was mildly reduced in three-quarters of the trials at 3 h and half the trials at 6 h, with values

ranging from 0.1 to 0.8 times that of the control strain in the same medium (Figure 7A). Pds1p is also reduced or enriched upon overexpression or depletion, respectively, of Cdc20p, in *S. cerevisiae* (Visintin et al., 1997; Raspelli et al., 2015), although the effects are more pronounced. Variability in Eip1p responses may reflect heterogeneity in the *C. albicans* Cdc20p-depleted cell phenotype (Chou et al., 2011) and/or other factors that contribute to Eip1p regulation.

To further investigate the hypothesis that Eip1p is regulated in part by degradation during mitosis, Eip1p was tagged with the TAP epitope in a strain carrying a single conditional copy of another mitotic regulator, the polo-like kinase *CDC5*. In *S. cerevisiae*, Pds1p is not affected by *CDC5* overexpression, but is reduced in
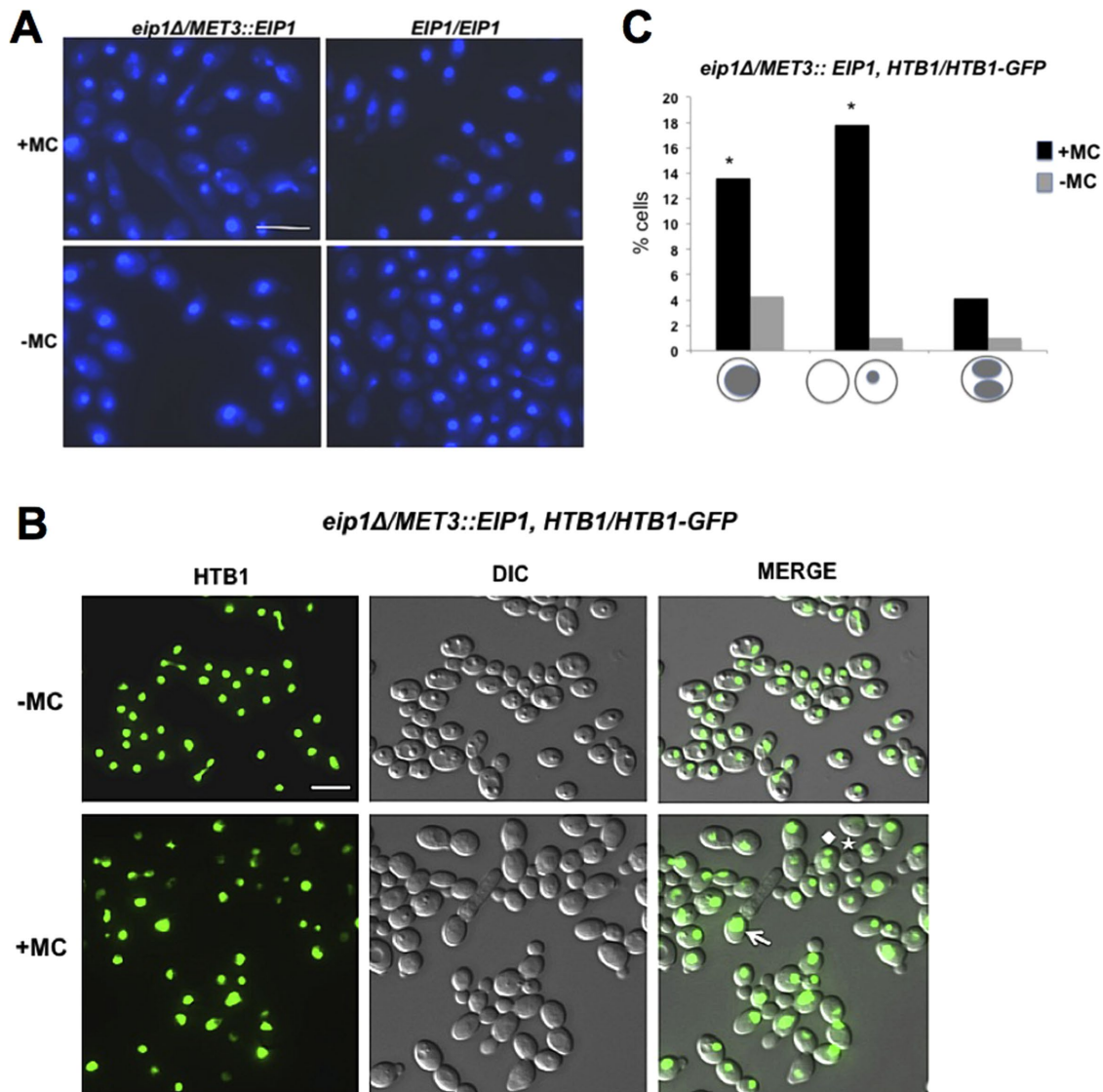

FIGURE 5: Cells depleted of Eip1p can segregate chromosomes but show multiple defects. (A) Strains SS25 (*eip1::URA3/MET3::EIP1-HIS1*) and BWP17 (*EIP1/EIP1*) were incubated in inducing (–MC) or repressing medium (+MC) for 8 h, fixed, and stained with DAPI. (B) Strain SS44 (*HTB1/HTB1-GFP-ARG4, eip1::URA3/MET3::EIP1-HIS1*) was incubated in –MC or +MC medium for 7 h, mounted, and imaged live. Abnormal features including two DNA masses within one cell (diamond), empty cell compartments (star), and large DNA masses (arrow) are indicated. (C) Proportions of cells in B containing enlarged DNA masses, fragments or no DNA, or two DNA masses within a single cell compartment. Sample sizes include 286 (+MC) and 277 (–MC) cells. Significance was measured with a Fisher exact test, two-tailed, where * indicates $p < 0.05$. (D) Time-lapse imaging of strain SS44 in –MC or +MC medium. Images were captured every 5 min for 180 min. Bars: 10 μm.

Continues.

D   *eip1Δ/MET3::EIP1, HTB1/HTB1-GFP*

-MC
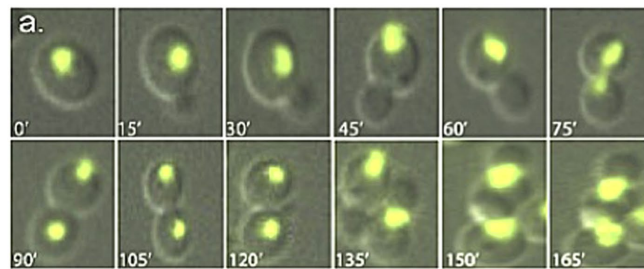
+MC
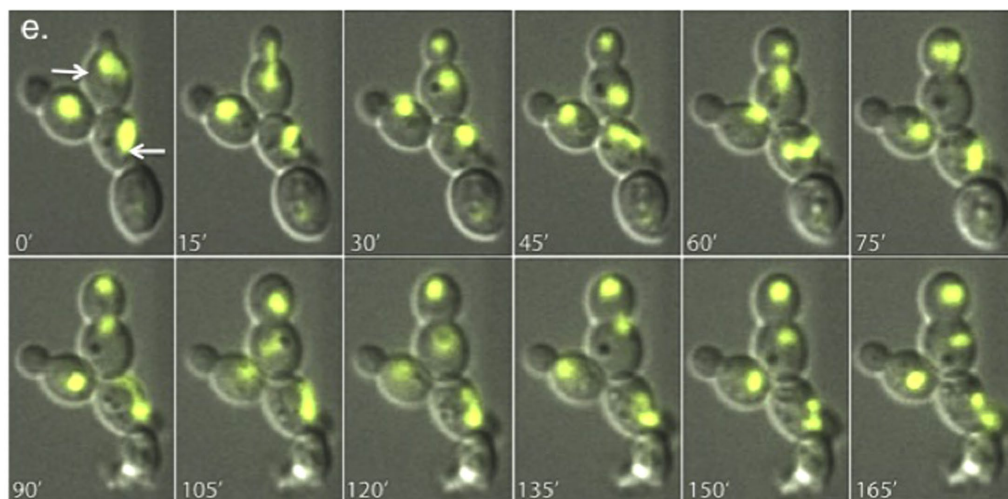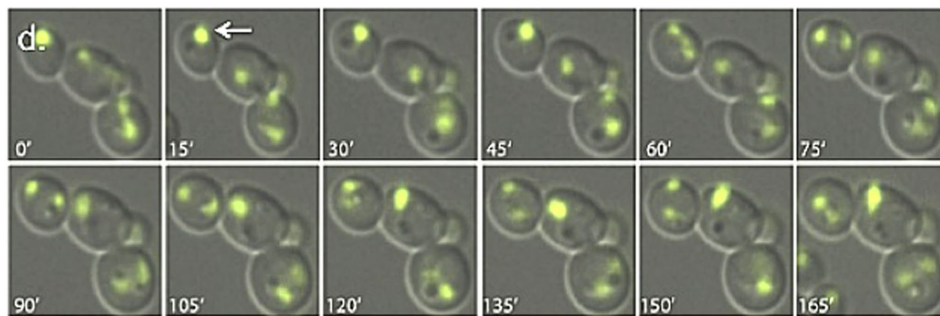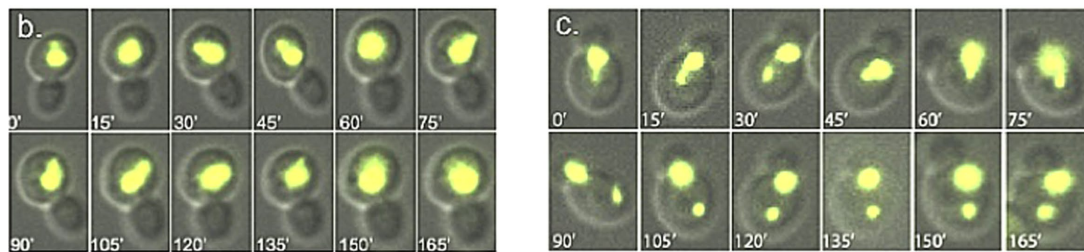
FIGURE 5: Continued.

the absence of Cdc5p due to the fact that cells arrest past the point when most Pds1p is degraded (Charles *et al.*, 1998). In *C. albicans*, Cdc5p depletion results in a phenotype similar to that described for Cdc20p-depleted cells (Figure 7D) (Bachewich *et al.*, 2003, 2005; Chou *et al.*, 2011). However, the precise initial arrest

point in either condition remains unclear. When cells were incubated in inducing medium to overexpress *CDC5*, the level of Eip1p was similar to that of the control strain (Figure 7C). However, upon depletion of Cdc5p in repressing medium, Eip1p-TAP was significantly and consistently reduced (Figure 7C). Thus, Eip1p is

turned over during a block in mitosis induced by Cdc5p depletion, but this does not occur in the absence of Cdc20p. This suggests that Cdc20p may be required in part for Eip1p degradation in mitosis, similar to other securins.

Eip1p increases in response to methyl methanesulfate (MMS) or hydroxyurea (HU) treatment, and is important for the metaphase arrest

The securin Pds1p in *S. cerevisiae* is essential for preventing anaphase initiation and mitotic exit in response to γ-irradiation–induced DNA damage in G2 or spindle defects. It is stabilized by phosphorylation in a Mec1p- and Chk1p-dependent manner and Mad2p-dependent sequestration of Cdc20p, respectively (Yamamoto *et al.*, 1996b; Cohen-Fix and Koshland, 1997; Sanchez *et al.*, 1999; Tinker-Kulberg and Morgan, 1999; Palou *et al.*, 2017). Pds1p is also stabilized in response to HU or MMS, but this is not sufficient to block cell cycle progression; *pds1Δ* cells remain arrested due to Swe1p and Rad53p-mediated down-regulation of mitotic CDK activity (Palou *et al.*, 2015, 2017). To determine whether Eip1p is important for a mitotic arrest during the response to DNA damage, cells containing Eip1p tagged with the MYC epitope were incubated in the presence or absence of MMS for 5 h, and processed for Western blotting. The mobility of Eip1p-MYC was not grossly affected by MMS, unlike the situation for Pds1p. We cannot rule out the possibility of undetectable phosphorylation under the current conditions, but it is noteworthy that Eip1p has only one CDK consensus phosphorylation site versus five in Pds1p (Agarwal and Cohen Fix, 2002). However, Eip1p levels were significantly enriched in response to MMS (Figure 8A).
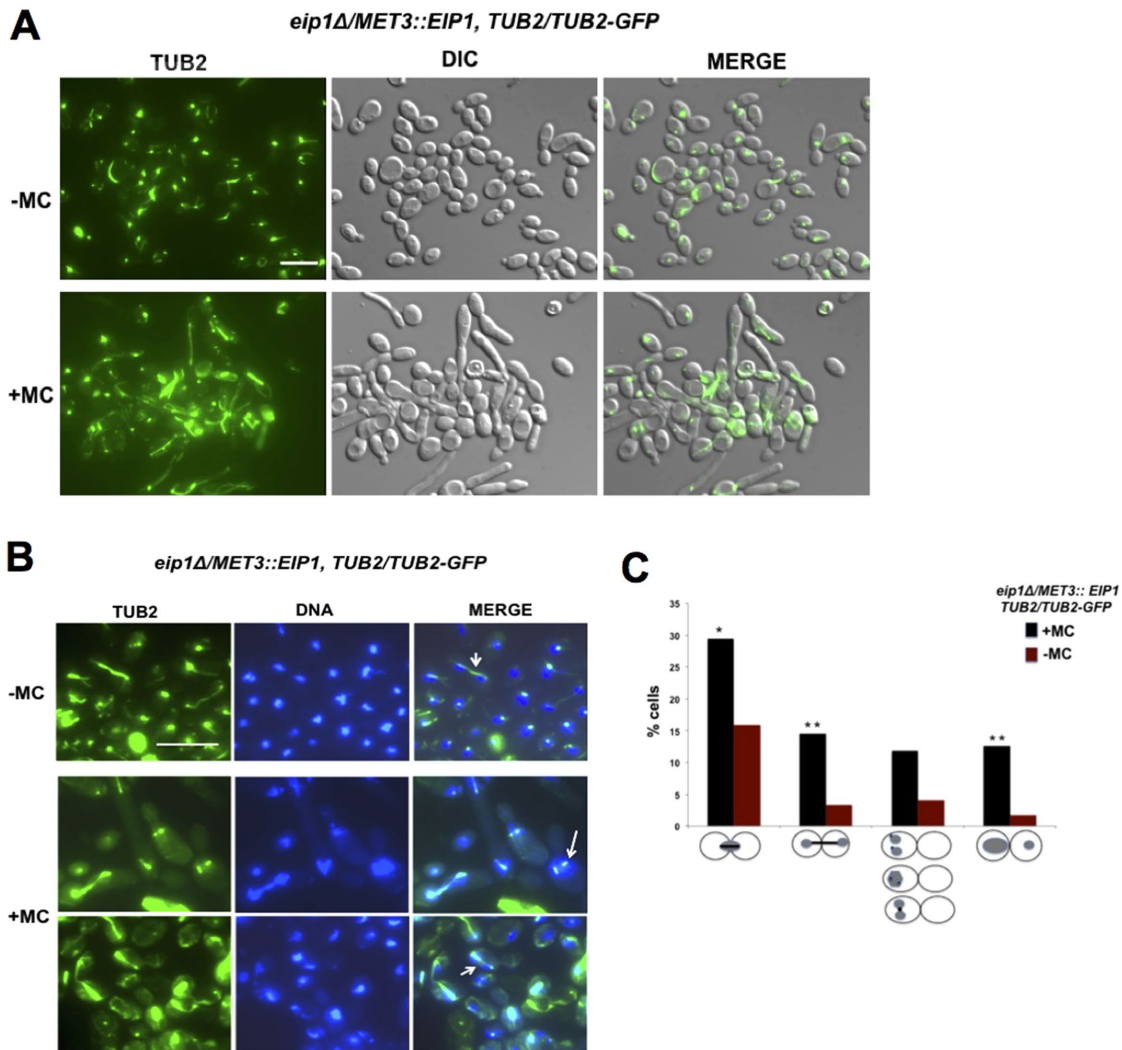

FIGURE 6: Eip1p depletion results in a higher proportion of cells with mitotic spindles. (A) Strain SS38 (*TUB2-GFP-ARG4/TUB2, eip1::URA3/MET3::EIP1-HIS1*) was incubated in inducing (–MC) or repressing medium (+MC) for 7 h and imaged live. (B). Strain SS38 was prepared as in (A), then fixed and stained with DAPI. Late anaphase spindles are designated by short arrows. The short arrow in the +MC condition also highlights a misoriented spindle and uneven chromosome segregation. The long arrow indicates two short spindles in a single DNA mass. (C) Proportions of cells in B with short spindles at the bud neck; elongated late anaphase spindles that spanned the mother and daughter cells; one DNA mass with two spindle pole bodies, two DNA masses in a single cell, either connected by a spindle or with separate spindle pole bodies; or uneven segregation of DNA between mother and daughter cell. Sample sizes include 387 (+MC) and 309 (–MC) cells. Significance was determined with a Fisher exact test, two-tailed, with *$p < 0.05$, **$p < 0.01$. (D) Time-lapse imaging of strain SS38 showing normal spindle formation and disassembly in –MC medium, or defects in +MC medium. Images were captured every 5 min for 180 min. Bars: 10 µm.
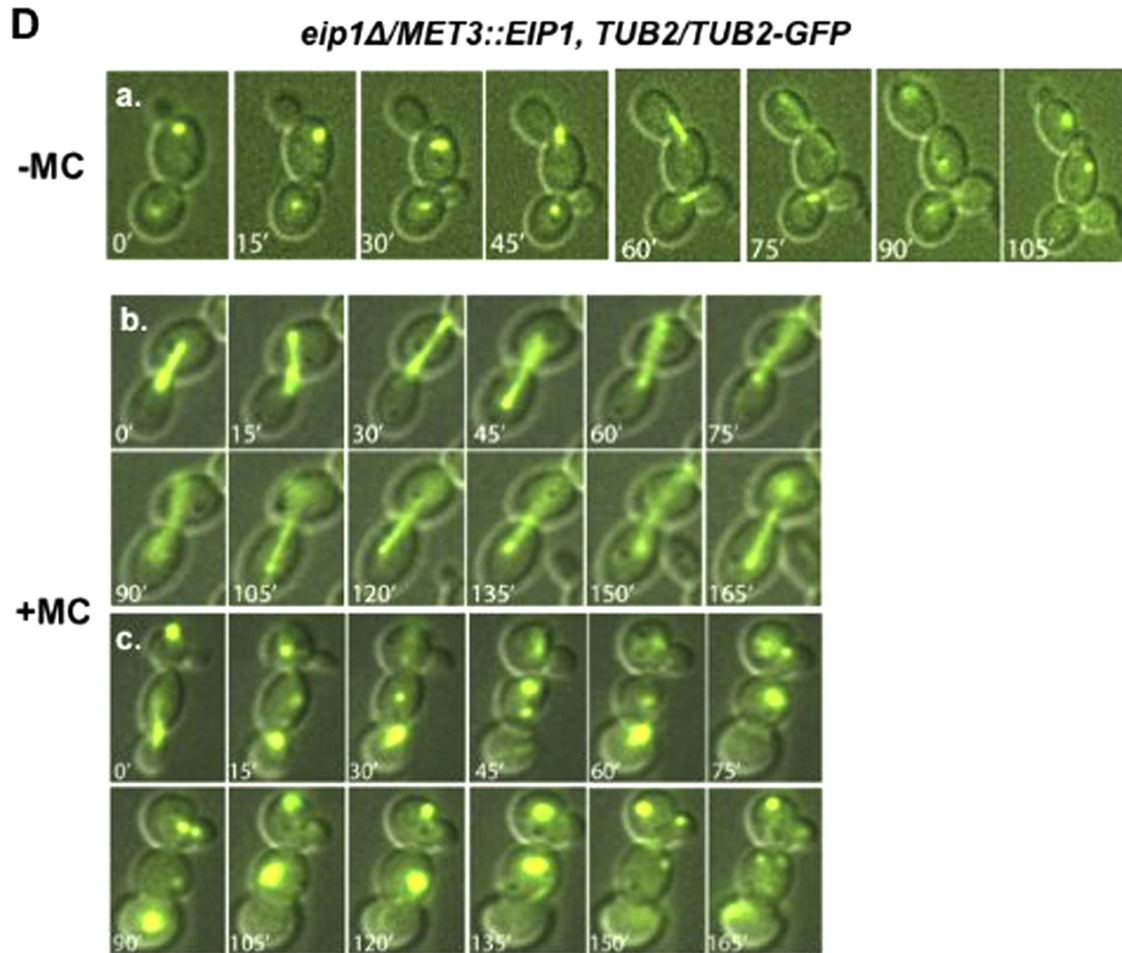
Continues.

D

eip1Δ/MET3::EIP1, TUB2/TUB2-GFP

-MC

+MC

FIGURE 6: Continued.

This may be due to a high proportion of cells blocked in early mitosis in response to MMS (Wang *et al.*, 2012; Figure 8C), or stabilization or induction of Eip1p. When the experiment was repeated with the exception of using 200 mM HU, Eip1p levels were also enhanced (Figure 8B). Thus, Eip1p is strongly enriched in response to DNA damage and replication stress.

If enrichment of Eip1p is important for mediating the MMS- or HU-induced arrest in mitosis, then absence of Eip1p may allow cells to progress through the block. To test this hypothesis, the *EIP1* conditional strain carrying a copy of *TUB2* tagged with GFP was incubated in inducing or repressing medium for 2.5 h, transferred to fresh media containing 0.02% MMS or 200 mM HU, incubated for 5 h, and then fixed and stained with DAPI. In the presence of Eip1p, the majority of MMS-treated cells demonstrated a very short spindle and localization of DNA near the bud neck (Figure 8, C and D). In the absence of Eip1p, however, the proportion of cells with this pattern was greatly reduced, and more cells were in later stages of mitosis (Figure 8, C and D). This contrasts to the situation in *S. cerevisiae Δpds1* cells, which remain arrested when treated with MMS or HU due to Swe1p and Rad53p-mediated down-regulation of mitotic CDK (Palou *et al.*, 2015, 2017). When incubated in HU, *C. albicans* cells responded similarly to when treated with MMS (Figure 8, E and F). The results suggest that Eip1p may be critical for blocking anaphase under conditions of MMS- or HU-induced DNA stress. The data provide additional support for Eip1p acting as a securin

and underscore unique features of the mitotic regulatory networks in *C. albicans*.

The cohesin homologue Mcd1p/Scc1p is reduced on depletion of Eip1p

Separase functions in part through cleaving the cohesin subunit Mcd1p/Scc1p for sister chromatid separation (Kumar, 2017). The cohesin complex has not been investigated in *C. albicans*, but *MCD1/SCC1* (*ORF19.7634*) is 34% identical to its homologue in *S. cerevisiae* (www.candidagenome.org/). If Eip1p is a securin that regulates separase, then modulation of Eip1p may influence the separase target Mcd1p. To investigate this, Mcd1p was tagged with TAP in an *EIP1*-conditional strain, cells were incubated in inducing or repressing medium for set times, and the levels of Mcd1p were determined by Western blotting. When Eip1p was depleted, Mcd1p was moderately reduced (Figure 9A), consistent with Eip1p having an inhibitory effect on separase. We next determined the levels of Mcd1p in Eip1p-depleted cells exposed to MMS. Since MMS arrests cells in early mitosis, and depletion of Eip1p under these conditions permits many cells to escape the arrest, we reasoned that Mcd1p should also be reduced. To test this, the *EIP1*-conditional strain carrying a TAP-tagged copy of *MCD1* was incubated in inducing or repressing medium for 2.5 h, transferred to fresh media containing 0.02% MMS or 200 mM HU, incubated for set times, and then fixed and stained with DAPI. Western blotting demonstrated that after 5 h
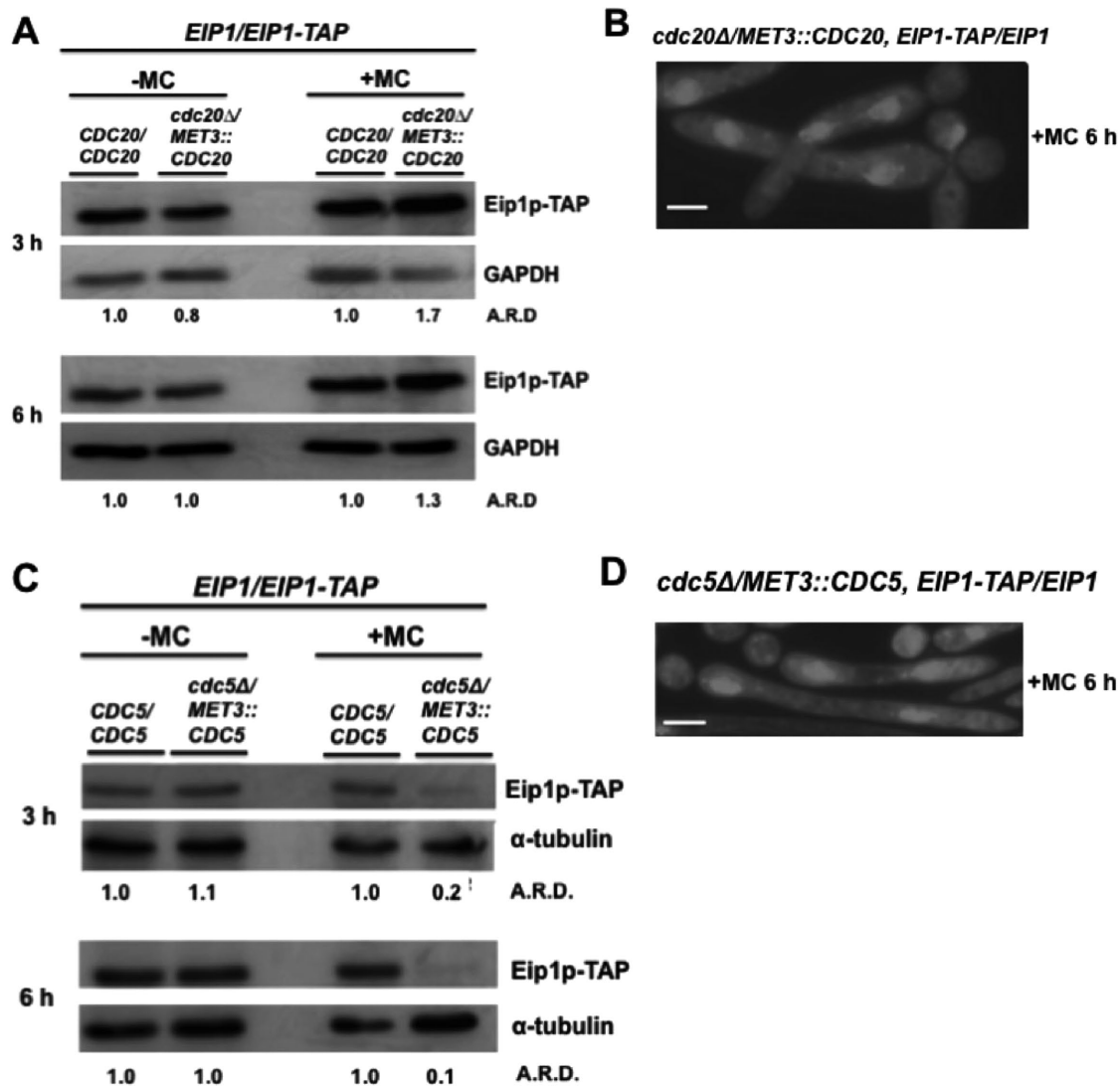
FIGURE 7: Eip1p is reduced in cells depleted of Cdc5p, but not Cdc20p. (A) Strains SS40 (*eip1::URA3/EIP1-TAP-ARG4*) and SS41 (*EIP1/EIP1-TAP-ARG4, cdc20::URA3/MET3::CDC20-HIS1*) were incubated in inducing (–MC) or repressing (+MC) medium. Samples were collected at 3 or 6 h and processed for Western blot analysis using anti-TAP antibody and anti-GAPDH antibodies. Adjusted relative densities (A.R.D.) of Eip1p-TAP bands were determined using strain SS40 in either –MC or +MC medium as a reference. (B) Strain SS41 incubated in +MC medium for 6 h, fixed, and stained with DAPI. (C) Strains SS40 and SS43 (*EIP1/EIP1-TAP-URA3, cdc5::hisG/ MET3::CDC5-ARG4*) were incubated and analyzed with Western blotting as described in A, with the exception of using anti–α-tubulin antibody as a loading control. (D) Strain SS43 was incubated in +MC medium for 6 h, fixed, and stained with DAPI. Bars: 5 µm.

of Eip1p depletion in the presence of MMS, Mcd1p was significantly reduced (Figure 9B). The data demonstrate that Eip1p can impact the levels of Mcd1p, a homologue of a cohesin subunit and target of separase, and support the model that Eip1p may function as a securin in *C. albicans*.

DISCUSSION

Proper chromosome segregation at the metaphase-to-anaphase transition is critical for maintaining genomic stability and is dependent on the highly conserved cohesin protease, separase. Securins are key regulators of separase, yet to date have been identified only in select model yeast, worms, flies, mice, and humans due to divergence in sequence (Moschou Bozhkov, 2012). *C. albicans* is a critical fungal pathogen of humans, and a deeper understanding of the regulation of its proliferation will be important for devising new strategies to treat infection. Through characterizing the *C. albicans*

separase homologue Esp1p, we identified Eip1p, a *Candida*-specific separase-interacting protein that is important for growth and a candidate new securin. Our results provide an approach for identifying these divergent proteins, reveal new insights on mitotic regulation in fungi, and identify a potential novel target for anti-fungal therapeutics.

Since securins are difficult to identify with sequence-based homology searches, we reasoned that a functional homologue in *C. albicans* may be revealed by determining the interacting proteins of the separase homologue, Esp1p. However, Esp1p first required characterization since its functions were not clear. Here, we provide the first demonstration that *C. albicans* Esp1p is important for chromosome segregation. Esp1p-depleted cells were large-budded with an unsegregated DNA mass. Many contained short spindles characteristic of G2/M or early anaphase, but few elongated late anaphase spindles. Finally, some cells contained extra spindle pole
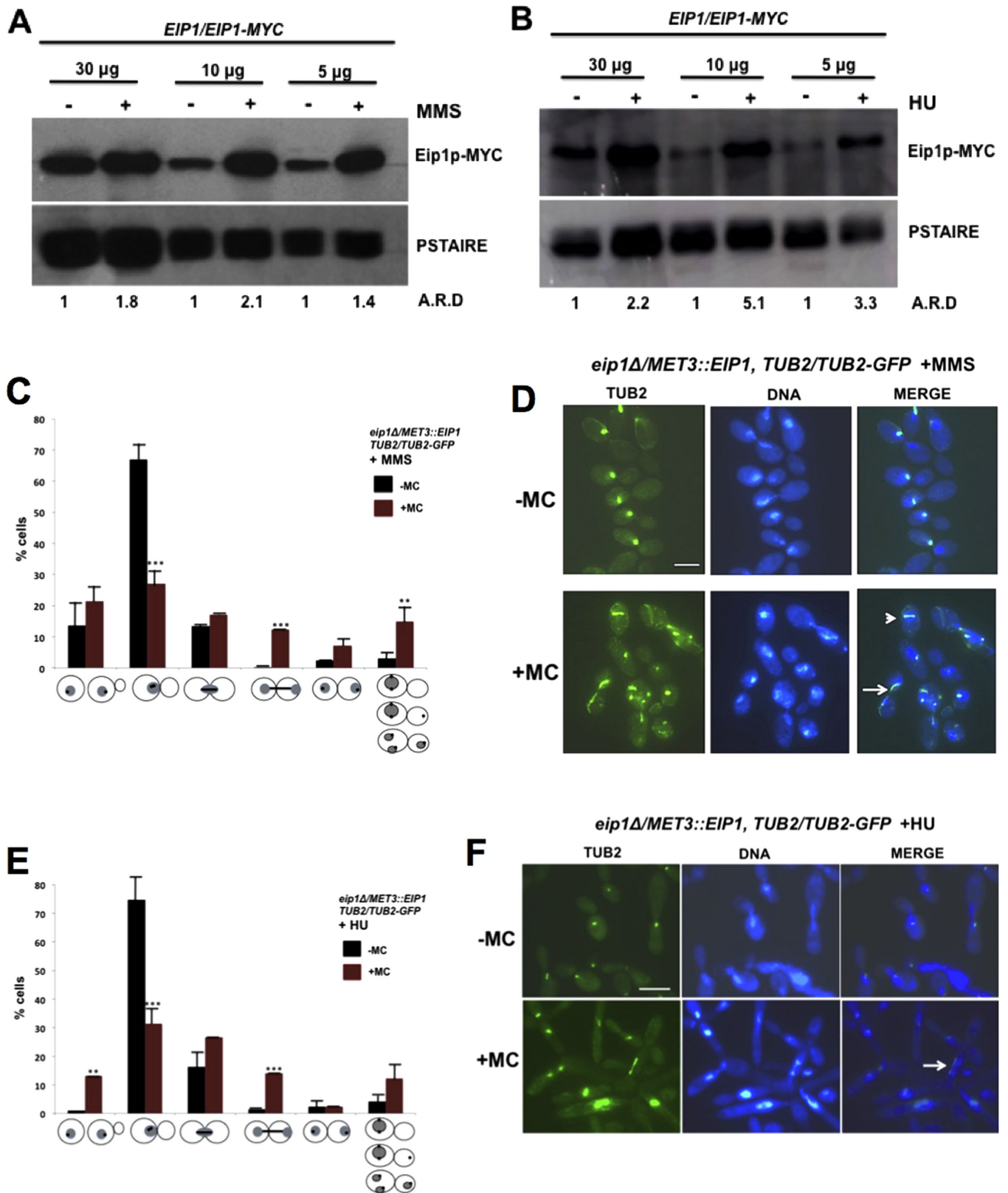
FIGURE 8: Eip1p is enriched in response to MMS or HU treatment, and its depletion permits cells to escape an MMS or HU-induced metaphase block. (A, B) Strain SS22 (*eip1::URA3/EIP1-MYC-HIS1*) was incubated in the presence or absence of 0.02% MMS or 200 mM HU for 5 h, collected, and processed for Western blotting. Treated (+) and untreated (–) samples (30, 10, or 5 μg) were loaded onto a 10% SDS gel. Blots were incubated with anti-MYC antibody, stripped, and then incubated in anti-pSTAIRE antibody. Adjusted relative densities (A.R.D.) of Eip1p-MYC bands were obtained using lanes of untreated samples as a reference for each amount of protein loaded. (C, D) Strain SS38 (*TUB2-GFP-ARG4/ TUB2, eip1::URA3/MET3::EIP1-HIS1*) was incubated in inducing (–MC) or repressing (+MC) medium for 2.5 h, transferred
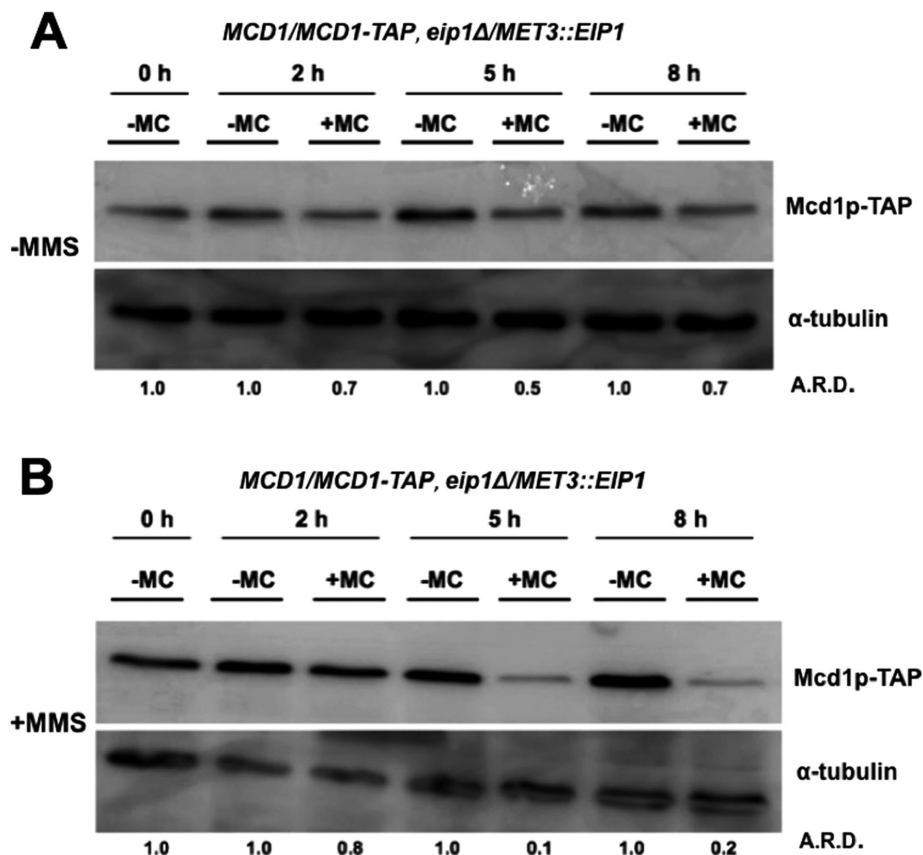
FIGURE 9: Cohesin subunit Mcd1p/Scc1p is reduced when Eip1p is depleted. (A) Strain SS84 (*MCD1-TAP-ARG4/MCD, eip1::URA3/MET3::EIP1-HIS1*) was incubated in inducing (–MC) or repressing (+MC) medium. Samples were collected at set times and processed for Western blot analysis. Blots were incubated with anti-TAP and anti–α-tubulin antibodies. Adjusted relative densities (A.R.D.) of Mcd1p-TAP bands were obtained using lanes from samples incubated in –MC medium as a reference for each time point. (B) Strain SS84 was incubated in –MC or +MC medium for 2.5 h, diluted into fresh –MC or +MC medium containing 0.02% MMS, and incubated for set times. Western blotting analysis was performed as described in A.

that activates partial release of the phosphatase Cdc14p from the nucleolus. However, Esp1p and Cdc14p in *S. cerevisiae* have been reported to interact in a genetic rather than physical manner (www.yeastgenome.org), and homologues of Cdc5p, Slk19p, and PP2A[Cdc55] did not copurify with Esp1p in *C. albicans*. Whether these differences reflect technical issues and/or diverse functional relationships remains to be determined. Notably, an equivalent FEAR pathway has not been identified in *C. albicans*. Collectively, the data are consistent with *C. albicans* Esp1p acting as a separase at the metaphase-to-anaphase transition. Given the diverse roles of separases (Kumar, 2017), Esp1p may have additional functions. Consistently, histones and histone deacetylase complex factors copurified with Esp1p from exponential phase *C. albicans* cells (unpublished data), suggesting possible roles in nucleosome organization and gene expression.

Among the proteins that interact with Esp1p, Eip1p represents a candidate divergent securin based on several features. First, it was one of the most enriched Esp1p-interacting proteins and unique in sequence. Second, its predicted 3D structure shares at least some similarity with securin Pds1p from *S. cerevisiae*. Third, Eip1p contains putative KEN and destruction boxes and is turned over in mitosis in part through a Cdc20p-dependent manner, based on significant reduction in Eip1p during mitotic arrest induced by depletion of Cdc5p but not Cdc20p, similar to Pds1p (Charles *et al.*, 1998; Hilioti *et al.*, 2001). Fourth, Eip1p is important for chromosome segregation. Chromosome missegregation events in Eip1p-depleted cells were pleiotropic and resulted in abnormal ploidy in some cases. Fifth, Eip1p is enriched in response to DNA damage or replication stress, and its absence permits a proportion of MMS- or HU-treated cells to escape an early mitotic arrest, consistent with a role in blocking anaphase. *S. cerevisiae* Pds1p is also stabilized in response to HU or MMS, but this is not sufficient to block cell cycle progression; *pds1Δ* cells remain arrested due to Swe1p and Rad53p-mediated

bodies within a single mass of DNA, consistent with continuation of the cell cycle and similar to the situation with Esp1p-depleted *S. cerevisiae* cells (Baum *et al.*, 1988; McGrew *et al.*, 1992). We also provide the first picture of putative Esp1p-interacting proteins in *C. albicans*. Cdc14p was one of the most enriched factors. Consistently, a recent screen for Cdc14p physical interactors in *C. albicans* identified Esp1p (Kaneva *et al.*, 2019). Esp1p in *S. cerevisiae* functions with Cdc5p, Slk19p and PP2A[Cdc55] as part of the FEAR pathway

to fresh –MC or +MC medium, respectively, containing 0.02% MMS, and incubated for 5 h. Cells were fixed and stained with DAPI. Proportions of cells showing different patterns of Tub2p-GFP associated with DAPI staining and cell bud stage were quantified. Tub2p-GFP appeared as a small spot associated with DNA in unbudded or small-budded cells representing a spindle pole body of G1/early S phase cells, a more intense spot in larger-budded cells with DNA confined to the mother cell reflecting S-G2/M phase cells, a short rod associated with a single mass of DNA representative of a metaphase or early anaphase spindle (arrowhead in D), an elongated bar with separated DNA masses at the ends reflecting late anaphase (arrow in D), or two separate spindle pole bodies associated with segregated DNA in large-budded cells, reflecting exit from mitosis. Abnormal organizations including two spindle pole bodies per DNA mass, or multiple DNA masses within one cell compartment were also observed. Error bars represent SD from the mean of biological duplicates. Sample sizes included at least 140 cells. Significance was determined using the Fisher exact test, two-tailed, with **$p < 0.01$ and ***$p < 0.001$. (E, F) Strain SS38 was incubated and analyzed as described in C and D, with the exception of using 200 mM HU. Error bars represent SD from the mean of biological duplicates. Sample sizes included at least 80 cells. Significance was determined using the Fisher exact test, two-tailed, with **$p < 0.01$ and ***$p < 0.001$. Bars: 10 μm.

down-regulation of mitotic CDK activity (Palou *et al.*, 2015, 2017). Intriguingly, the absence of Rad53p in *C. albicans* allows progression through an MMS-induced G2/M block (Shi *et al.*, 2007), unlike the situation in *S. cerevisiae* (Palou *et al.*, 2015), underscoring differences in the mechanisms governing mitotic progression between the two organisms. Finally, Eip1p modulates the levels of Mcd1p/Scc1p, a homologue of the separase target cohesin. Collectively, the data support the hypothesis that Eip1p functions as a securin-like protein. To confirm whether Eip1p shares additional traits of securins, investigation of its cell cycle-regulated abundance, functionality of its putative KEN and destruction boxes, and its ability to block mitosis when in a nondegradable form should be explored.

Eip1p-depleted cells demonstrated other phenotypes that were distinct and may reflect additional functions. For example, the presence of misoriented spindles, a stretched and misoriented DNA mass in the mother cell that subsequently reoriented and segregated to the daughter cell, or two separate DNA masses within one cell compartment, implies a role for Eip1p in spindle orientation. Intriguingly, similar phenotypes were reported for mutants of Kar9p in *S. cerevisiae* (Miller and Rose, 1998) and dynein in *C. albicans* (Finley *et al.*, 2008). Kar9p in *S. cerevisiae* mediates a connection between the plus end of astral microtubules associated with one spindle pole body and type V myosin on cortical actin cables. Coupled with depolymerization of the microtubules at the cortex, this moves the nucleus to the bud neck. The spindle oscillates across the neck via dynein acting on astral microtubules and subsequent spindle elongation at anaphase partitions the DNA between mother and daughter cells (Gladfelter and Berman, 2009). Thus, Eip1p may impact spindle orientation through a mechanism affecting cortical positioning cues, microtubule dynamics/integrity, or associated motors. Consistently, some abnormalities in microtubules and spindles were observed in Eip1p-depleted cells, as well as random oscillations of elongated spindles and abnormal movements of nuclei, at times from mother cell to bud and back. The latter, particularly reverse movement of the postmitotic nucleus back to the mother cell, is highly unusual for yeast and the mechanisms remain unclear. In hyphae, retrograde movement of a daughter nucleus to the mother cell after division in the germ tube is accomplished by spindle elongation, but a slower and unknown mechanism is required after the spindle disassembles (Finley and Berman, 2005). Another distinct phenotype included maintenance of elongated spindles. Where spindles were confined to the mother cell, it is possible that the spindle orientation checkpoint was activated by spindle disorientation and/or cytoplasmic microtubule defects, which delays mitotic exit and spindle disassembly (Finley *et al.*, 2008; Caydasi *et al.*, 2010). Down-regulation of some MEN factors in *S. cerevisiae* can also impair spindle orientation through affecting Kar9p localization (Hotz *et al.*, 2012). However, maintained spindles in other Eip1p-depleted cells spanned the mother and daughter cells, reminiscent of spindle disassembly or MEN pathway mutants (Woodruff *et al.*, 2010; Weiss 2012). In *C. albicans*, these pathways are not well defined (Bates, 2018). Further, *C. albicans* homologues of some *S. cerevisiae* MEN factors, including Dbf2p and Cdc14p, have prominent functions in additional processes (Clemente-Blanco *et al.*, 2006; González-Novo *et al.*, 2009). Intriguingly, Dbf2p shares several phenotypes with Eip1p (González-Novo *et al.*, 2009). In *S. cerevisiae*, *pds1Δ* cells did not demonstrate a spindle maintenance phenotype. Rather, some cells were multinucleate, consistent with precocious mitotic exit due to the positive role for separase in this process and inhibition by Pds1p (Hatano *et al.*, 2016). Although two DNA masses were also present in some Eip1p-depleted cells, they were often connected by a spindle. Coupled with other microtubule-

dependent processes affected, we propose that maintenance of elongated spindles in a proportion of Eip1p-depleted cells may be due to an impact on spindle disassembly mechanics, as opposed to Eip1p playing some positive role in the mitotic exit pathway. It is possible that the additional phenotypes involving spindle behavior and/or microtubules in Eip1p-depleted cells may be indirect effects of deregulated separase, since separases are important for a variety of spindle-related processes (Kumar, 2017). Alternatively, we cannot rule out the possibility that they represent separase-independent functions of Eip1p. Consistently, the securin Pttg1 has several roles, including a separase-independent function in microtubule nucleation (Moreno-Mateos *et al.*, 2011). Taken together, we propose that Eip1p may function as a securin that regulates separase for chromosome segregation and may have additional roles that impact spindle orientation, disassembly, and/or microtubule function. In this way, Eip1p could coordinate multiple aspects of mitotic progression.

Chromosome segregation and cell division could take place in many cells lacking Eip1p, suggesting that Eip1p may not be immediately essential for these processes. While it is possible that trace amounts of Eip1p were present, or that deletion strains contained secondary mutations that permitted growth, it is notable that diverse phenotypes were observed within groups of closely associated Eip1p-depleted cells. In addition, repressing *EIP1* with the *TET* versus *MET3* promoter produced similar effects, *eip1Δ/Δ* cells from independent transformations resembled cells depleted of Eip1p, and depletion of Esp1p using the *TET* or *MET3* promoter resulted in more severe and homogeneous effects on growth and chromosome segregation than depletion of Eip1p. We propose that cells lacking Eip1p variably accumulate defects in chromosome segregation, which can lead to a loss in viability, somewhat similar to the situation with *EST* mutants in *S. cerevisiae* (Lundblad and Szostak, 1989). Where securins are essential, the null phenotype resembles that of separase mutants due to the negative and positive regulation of separase by securin (Funabiki *et al.*, 1996; Hellmuth *et al.*, 2015). If securin is not essential, separase requires additional negative regulation. In metazoans, CDK/cyclin B phosphorylation serves this role (Hellmuth *et al.*, 2015). In *S. cerevisiae*, Slk19p and PP2A^{Cdc55} act redundantly with Pds1p to negatively regulate Esp1p (Lianga *et al.*, 2018). *C. albicans* has homologues of Slk19p and Cdc55p, but they are not characterized. Since several mitotic factors show variations in function in *C. albicans*, different proteins could contribute to separase regulation. Eip1p may be even more critical for chromosome segregation under specific conditions, including DNA damage or replication stress caused by MMS or HU treatment, respectively.

In summary, we identified a separase-binding protein, Eip1p, with functions that suggest that it is a new candidate securin. Our work provides an approach for identifying divergent securins and expands our understanding of the factors involved in regulating the metaphase-to-anaphase transition in eukaryotic cells. Given its importance in cell division, and lack of a sequence homologue in humans, Eip1p also represents a candidate target for approaches aimed at controlling growth of *C. albicans*. Determining the full range of functions and regulation of Eip1p and separase in *C. albicans* will provide additional important insights on the circuitry controlling fungal cell proliferation and diversity in eukaryotic mitotic networks.

MATERIALS AND METHODS
Strains, oligonucleotides, plasmids, and culture conditions
Strains, oligonucleotides, and plasmids used in this study are listed in Supplemental Tables S1–S3, respectively. Strains were cultured in

rich media (YPD) containing 1.0% yeast extract, 2.0% peptone, 2.0% glucose, and 50 µg/ml uridine (Bensen et al., 2002). Alternatively, strains containing genes under control of the MET3 promoter were incubated in synthetic defined yeast culture medium containing 0.67% of yeast nitrogen base, 2.0% dextrose, and amino acid supplements (2.0 g adenine, 2.5 g uridine, 2.0 g tryptophan, 1.0 g histidine, 1.0 g arginine, 1.5 g tyrosine, 1.5 g isoleucine, 7.45 g valine, 1.5 g lysine, 2.5 g phenylalanine, 5.0 g glutamic acid, 10.0 g threonine, and 3.0 g leucine per 50 l) that either lacked methionine and cysteine for promoter induction (–MC) or contained 2.5 mM methionine and cysteine for promoter repression (Care et al., 1999). For TET-regulated strains, cells were incubated in YPD medium with or without 100 µg/ml doxycycline hyclate (Sigma-Aldrich). Uridine, histidine, and/or arginine were omitted under conditions of prototroph selection. For growth assays or protein extraction, overnight cultures of cells were diluted into fresh medium to an OD_{600nm} of 0.1 or 0.2 and collected after incubation at either an OD_{600nm} of 0.8–1.0 or at the indicated time points. Alternatively, cells from plates were mixed in small volumes of liquid media, from which large dilutions were made. Cultures that were in low exponential phase the next day were then collected and diluted into fresh medium to an OD_{600nm} of 0.1 or 0.2 for subsequent incubation as described. For colony growth assays on solid media, overnight cultures of cells were washed in water, diluted to an OD_{600nm} of 0.1, serial diluted (100×), and spotted (4.0 µl) on plates. For affinity purification of Esp1p-TAP in a CDC20 conditional background, strains were incubated overnight in inducing medium, diluted to an OD_{600nm} of 0.4 in repressing medium, and collected after 4 h incubation. To measure the levels of Eip1p-MYC in response to MMS or HU, overnight cultures were diluted to an OD_{600nm} of 0.1 in YPD medium containing 0.02% MMS (Sigma-Aldrich), 200 mM HU (Sigma-Aldrich), or no drug and incubated for 5 h. Cells were then collected and processed for Western blotting. To determine the effects of MMS or HU on cells with or without Eip1p, low exponential cultures of strains were diluted into fresh inducing or repressing medium at a starting OD_{600nm} of 0.25, incubated for 2.5 h, collected, diluted into fresh inducing or repressing medium containing 0.02% MMS or 200 mM HU, and incubated for a further 5 h before fixation. Unless otherwise noted, all experiments were performed at 30°C and repeated at least two times.

Strain construction

To tag the C-terminus of ESP1 with the TAP epitope (protein A and calmodulin-binding protein separated by a TEV protease cleavage site) (Lavoie et al., 2008), the 3.0-kb TAP-URA3 cassette was amplified from plasmid pFA-TAP-URA3 (Lavoie et al., 2008) with primer pair AG103F and AG103R. The 3.0-kb construct was transformed into strain BWP17, resulting in strain AG636. Correct integration was confirmed using primer pair AG104F and AG3R. The second copy of ESP1 was replaced using a two-step PCR. Primer pairs SS1F, SS1R and SS2F, SS2R were used to amplify sequences lying upstream from the START or downstream from the STOP codon for ESP1, respectively. The HIS1 cassette fragment from plasmid pBS-CaHIS1 (Chou et al., 2011) was amplified with primers SS3F and SS3R. The products were combined in a fusion PCR with primer pair SS1F and SS2R. The fusion construct was transformed into strain AG636 resulting in strain SS1. Correct integration was confirmed using PCR with primer pair SS10F and CaHIS1R. Transformant genomic DNA was extracted according to Rose et al. (1990). To tag ESP1 with TAP in a CDC20 conditional strain, the approach described above was used, and the product was transformed into strain HCCA109 (Chou et al., 2011) resulting in strain SS3. To create a strain containing a

single copy of ESP1 under control of the MET3 promoter, one copy of ESP1 was deleted from strain BWP17 using the strategy described previously, with the exception of amplifying the URA3 cassette from pBS-CaURA3 with primer pair SS3F and SS3R, resulting in strain SS20. Correct integration was confirmed with primer pairs SS10F and CaURA3R. Primer pairs SS19F, SS19R and SS20F, SS20R were used to amplify sequences upstream and downstream of the ESP1 START codon, respectively, while primers SS21F and SS21R amplified a HIS1-MET3 fragment from the pFA-MET-CaHIS1 plasmid (Gola et al., 2003). The three fragments were combined in a fusion PCR with primers SS19F and SS20R. The final construct was transformed into strain SS20 resulting in strain SS35. Correct integration was confirmed using primers SS26F and CaHIS1R. To tag the C-terminus of ESP1 with three copies of the hemaglutinin epitope (HA), a HA-URA3 cassette was amplified from plasmid pFA-HA-URA3 (Lavoie et al., 2008) with primers AG4F and AG4R. The product was used as a template in a fusion PCR with primers AG103F and AG103R. The fusion construct was transformed into strain BWP17 resulting in strain SS16. Correct integration was confirmed using primer pair CaURA3F and AG104R.

For creating a strain containing a single copy of EIP1 under the control of the MET3 promoter, primer pairs SS22F, SS22R and SS23F, SS23R were used to amplify sequences lying upstream from the EIP1 START codon or downstream from the STOP codon, respectively. Primer pair SS24F and SS24R amplified the URA3 cassette from the pBS-URA3 plasmid. The three fragments were combined in a fusion PCR with primers SS22F and SS23R. The final product was transformed into strain BWP17, resulting in strain SS10. Correct integration of product was confirmed by PCR with primers caURA3F and SS25R. To place the second copy of EIP1 under the control of the MET3 promoter, primer pairs SS27F, SS27R and SS28F, SS28R were used to amplify sequences lying upstream and downstream of the EIP1 START codon, respectively, while primers SS29F and SS29R amplified a HIS1-MET3 fragment from the pFA-MET-CaHIS1 plasmid. The three fragments were combined in a fusion PCR with primers SS27F and SS28R. The final construct was transformed into strain SS10 resulting in strain SS25. Correct integration of the construct was confirmed by PCR with primers SS25F and caHIS1R. To create a strain lacking both copies of EIP1, the remaining allele of EIP1 in strain SS10 was replaced as described for SS10, with the exception of amplifying a HIS1 cassette from pBS-HIS1 with primers SS24F and SS24R. The final fusion PCR product was transformed into strain SS10 resulting in strains SS63–65. Strains were confirmed with primer pairs CaURA3F/CaHIS1F and SS25R to confirm allele replacements with HIS1 and URA3, as well as SS25F and SS25R to screen for the presence of the EIP1 ORF. To construct a strain that contained a single copy of EIP1 tagged at the C terminus with the TAP epitope, the TAP-ARG4 cassette was amplified from plasmid pFA-TAP-ARG4 with primers SS33F and SS33R and transformed into strain SS10. The resulting strain SS40 was confirmed by PCR with primer pair CaARG4F and SS25R. A similar approach was used to tag EIP1 with TAP in strain HCCa23, resulting in strain SS41. Alternatively, EIP1 was tagged with TAP in strain AG500 by amplifying a TAP-URA3 construct from pFA-TAP-URA3 as described, resulting in strain SS43. To tag the C-terminus of EIP1 with 13 copies of the MYC epitope (Bensen et al., 2005), a MYC-HIS1 cassette was amplified from plasmid pMG2093 with oligonucleotides SS18F and SS18R. The product was transformed into strain SS10 resulting in strain SS22, or strain SS16 resulting in strain SS29. Correct integration of the PCR product was confirmed with primer pair CaHIS1F and SS25R.

To tag the C-terminus of TUB2 with the GFP, the GFP-ARG4 cassette (Gola et al., 2003) was amplified from plasmid pFA-GFP-ARG4

with primer pair CB135F and CB135R. The final fragment was transformed into strains SS25 and SS35, resulting in strains SS37 and SS38, respectively. To tag the C-terminus of *HTB1* with the GFP epitope, the *GFP-ARG4* cassette was amplified from plasmid pFA-GFP-*ARG4* with primers SS37F and SS37R. The construct was transformed into strain SS25, resulting in strain SS44. Strains were screened for protein expression using epifluorescence microscopy.

To tag the C-terminus of *MCD1* with the with the TAP epitope, the 3.0-kb *TAP-ARG4* cassette was amplified from plasmid pFA-TAP-*ARG4* with primer pair SS47F and SS47R. The 3.0-kb construct was transformed into strain SS25, resulting in strain SS86. Correct integration was confirmed using primer pair SS48F and SS48R.

Protein extraction and Western blotting

To measure the levels of Eip1p in response to manipulation of Cdc20p or Cdc5p, cells were collected as indicated above. Protein extracts were prepared using HK buffer according to Liu *et al.* (2010). Extracted protein was quantified using the Bradford assay (Bio-Rad, Mississauga, Canada). Briefly, 30 µg of protein was loaded onto SDS–PAGE gels and proteins were transferred to a polyvinylidene difluoride membrane (Bio-Rad). Membranes were blocked with Tris-buffered saline Tween (TBST; Tris [pH 7.5], 137 mM NaCl, 0.1% Tween 20) containing 5% skim milk for 1.5 h. Blots were washed 3× for 15 min in TBST, incubated for 2 h in 0.2 g/ml anti-TAP antibody (Thermo Scientific), and diluted in TBST. Blots were rinsed 3× for 15 min in TBST and incubated for 1 h in a 1/10,000 dilution of horseradish peroxidase–conjugated anti-rabbit secondary antibody (Santa Cruz). After washing, blots were developed using the Amersham ECL Western blotting analysis system (GE Healthcare). Blots were stripped and incubated with 1.0 µg/ml anti-GAPDH (Protein Tech) or 1/1000 dilution of anti–α-tubulin (Sigma-Aldrich) antibodies as a loading control. For detecting Esp1p-HA or Eip1p-MYC, membranes were incubated for 2 h in either 0.4 g/ml anti-HA antibody (12CA5; Roche) or 1.0 µg/ml anti-MYC antibody (Santa Cruz) diluted in TBST. Secondary antibodies including horseradish peroxidase-conjugated anti-mouse (KPL) or anti-rabbit (Santa Cruz) were diluted 1/10,000. Anti-PSTAIRE (Santa Cruz Biotechnology) was used as a loading control at 0.2 µg/ml. Western blots were quantified using ImageJ as described previously (Chou *et al.*, 2011).

Coimmunoprecipitation and affinity purification

For coimmunoprecipitation assays, overnight cultures of cells were diluted into 2.0 l of YPD medium and incubated at 30°C until the OD_{600nm} reached 0.8–1.0. The culture was centrifuged for 5 min at 3000 rpm, and the remaining pellet was immersed in dry ice and stored at –80°C. Protein was extracted as described above. Coimmunoprecipitation was performed according to Lavoie *et al.* (2008). Briefly, 40 µl of Mono HA 11 Affinity beads (Covance) was centrifuged at 1500 × *g* for 2 min at 4°C, washed 3× with 500 µl of HK buffer (Liu *et al.*, 2010), and centrifuged again. Beads were then added to 40 mg of protein extract, and samples were incubated overnight at 4°C with rocking. After centrifugation, the supernatant was transferred to fresh Eppendorf tubes. Beads were washed 5× with 1.0 ml of HK buffer, centrifuged, and resuspended in 500 µl of buffer. The contents were transferred to fresh Eppendorf tubes and centrifuged to pellet the beads. The supernatant was removed and protein was eluted by boiling in 50 µl of 1× SDS sample buffer (50 mM Tris, pH 6.8, 2% SDS, 0.01% bromophenol blue, 10% glycerol, 100 mM dithiothreitol [DTT]) for 10 min. After centrifugation, the supernatant was removed and beads were boiled in 40 µl of 1× SDS sample buffer for 10 min. Eluted samples were loaded on 7.5 or 10% SDS–PAGE gels for Western blotting. Affinity purification

assays were carried out according to Rigaut *et al.* (1999) and Liu *et al.* (2010). Briefly, cultures from strains AG153 and SS3 were prepared as described above, and 4 l resulted in 330 mg of input protein. Protein was precleared by adding 500 µl of prewashed Sepharose 6B beads (Sigma) (1:1 slurry in HK buffer) and rocking at 4°C for 30 min. After removing beads, protein extracts were incubated with prewashed immunoglobulin G Sepharose 6 Fast Flow (GE Healthcare) (1:1 slurry in HK buffer; 250 µl bead volume) overnight at 4°C. The extract and beads were poured into a Poly-Prep Chromatography Column (Bio-Rad). The eluate was discarded and beads were washed twice with 10 ml ice-cold IPP300 buffer (25 mM Tris-HCl, pH 8.0, 300 mM NaCl, 0.1% NP-40), twice with 10 ml IPP150 buffer (25 mM Tris-HCl, pH 8.0, 150 mM NaCl, 0.1% NP-40) and once with 10 ml TEV-CB (25 mM Tris-HCl, pH 8.0, 150 mM NaCl, 0.1% NP40, 0.5 mM EDTA, and 1 mM DTT). After adding 1.0 ml of TEV CB buffer containing 10 U of Ac-TEV protease (Invitrogen), the column was rocked overnight at 4°C. The eluate was collected and beads were washed with another 1.0 ml TEV CB buffer. To the final 2.0 ml eluate, 3.0 ml of CBB (25 mM Tris-HCl, pH 8.0, 150 mM NaCl, 1 mM Mg acetate, 1 mM Imidazole, 2 mM $CaCl_2$), 24.0 µl of 1.0 M $CaCl_2$, and 300 µl of Calmodulin Sepharose 4B (GE Healthcare) was added. The mixture was rocked for 1 h at 4°C. After centrifugation, beads were washed twice with 1.0 ml CBB (0.1% NP-40) and once with 1.0 ml CBB (0.02% NP-40). Protein was eluted by two subsequent additions of 1.0 ml CEB (25 mM Tris-HCl, pH 8.0, 150 mM NaCl, 0.02% NP-40, 1 mM Mg acetate, 1 mM Imidazole, 20 mM EGTA, 10 mM β-mercaptoethanol). The elutions were combined and protein was precipitated by adding 25% volume of 50% trichloroacetic acid. The samples were kept on ice for 30 min and then centrifuged for 10 min at 4°C. The supernatant was removed, and 1.0 ml of 80% acetone was added to wash the precipitate. The contents were then centrifuged for 10 min at 4°C to remove the acetone, and the sample was dried on ice for 60 min. The pellet was resuspended in 30 µl 1× SDS sample buffer and boiled for 10 min. Samples were loaded on an SDS–PAGE gel and run on gels until just entering the resolving gel (Liu *et al.*, 2010). The gel was stained with Coomassie blue (Bio-Rad), and gel pieces from tagged and untagged strains were cut and sent for analysis via Orbitrap LC/MS (IRIC, University of Montreal). Bands were destained in 50% MeOH (Sigma-Aldrich). Each band was shrunk in 50% acetonitrile (ACN), reconstituted in 50 mM ammonium bicarbonate with 10 mM TCEP (Tris[2-carboxyethyl] phosphine hydrochloride; Thermo Fisher Scientific), and vortexed for 1 h at 37°C. Chloroacetamide (Sigma-Aldrich) was added for alkylation to a final concentration of 55 mM. Samples were vortexed for another hour at 37°C. One microgram of trypsin was added, and digestion was performed for 8 h at 37°C. Peptide extraction was conducted with 90% ACN. The extracted peptide samples were dried down and solubilized in 5% ACN-0.2% formic acid (FA). The samples were loaded on a homemade C_{18}precolumn (0.3-mm inside diameter [i.d.] by 5 mm) connected directly to the switching valve. They were separated on a homemade reversed-phase column (150 µm i.d. × 150 mm) with a 56-min gradient from 10 to 30% ACN-0.2% FA and a 600-2nl/min flow rate on a Nano-LC-Ultra-2D (Eksigent, Dublin, CA) connected to an Q-Exactive Plus (Thermo Fisher). Each full MS spectrum acquired at a resolution of 70,000 was followed by 12 tandem-MS (MS-MS) spectra on the most abundant multiply charged precursor ions. Tandem-MS experiments were performed using collision-induced dissociation at a collision energy of 25%. The data were processed using PEAKS 8.5 (Bioinformatics Solutions, Waterloo, ON) and a concatenated *C. albicans* database. Mass tolerances on precursor and fragment ions were 10 ppm and 0.01 kDa, respectively. Variable selected posttranslational modifications were carbamidomethyl (C),

oxidation (M), deamidation (NQ), and phosphorylation (STY). The data were visualized with Scaffold 4.3.0 (protein threshold, 99%, with at least two peptides identified and a false-discovery rate of 0.1% for peptides).

Cell imaging

To visualize DNA, cells were fixed in fresh 70% ethanol for 20 min, washed with sterile water, incubated in 1.0 µg/ml (DAPI; Sigma-Aldrich) for 20 min, washed twice with sterile water, and mounted on slides. For visualization of *TUB2-GFP* or *HTB1-GFP* in living cells, cultures were diluted into repressing or inducing medium, incubated for set times, centrifuged at 3000 rpm for 3 min, washed twice in water, and mounted on regular slides. To determine cell viability, cells were stained with 10 µg/ml propidium iodide (Sigma-Aldrich) as previously described (Bachewich *et al.*, 2003). Cells were imaged on a LeicaDM6000B microscope (Leica Microsystems Canada, Richmond Hill, ON, Canada) equipped with a Hamamatsu-ORCA ER camera (Hamamatsu Photonics, Hamamatsu City, Japan) and the HCX PL APO 63× NA 1.40-0 oil or HCX PLFLUO TAR 100× NA 1.30-0.6 oil objectives. Differential Interference Contrast (DIC) optics, or epifluorescence with DAPI (460 nm), fluorescein isothiocyanate (500 nm), or Texas Red (615 nm) filters were utilized. Images were captured with Volocity software (Improvision, Perkin-Elmer, Waltham, MA). Alternatively, time-lapse imaging of Htb1p-GFP or Tub2p-GFP was performed by diluting overnight cultures of cells into inducing or repressing medium to OD_{600nm} 0.1 and incubating for 5 h. Cells were diluted 100-fold and transferred to an eight-well µSlide (Ibidi) containing similar media. Cells were imaged on a Nikon TI microscope equipped with a Photometrics Evolve 512 camera using a 63× objective (NA1.4) with the optical path defined for DIC and GFP (488 nm ex/550 nm longpass emission filters). Images were captured every 5 min for 3 h using NIS Elements software.

Bioinformatic analysis

Comparative analysis of the amino acid sequence of *ESP1* began with the alignment of its sequence alongside the sequences of Esp1 (*S. cerevisiae*), Cut1 (*S. pombe*), Sep-1 (*C. elegans*), and Espl-1 (*H. sapiens*) using ClustalW (Larkin *et al.*, 2007). Aligned sequences obtained from ClustalW were further analyzed using ESPript software (Robert and Gouet, 2014). Parameters used included sequence similarity (% similarity), alignment output layout (flashy, portrait), and a global score of 0.7, as set by the program. Analysis of the amino acid sequence of *EIP1* was completed as described for *ESP1* using Pds1 (*S. cerevisiae*), Cut2 (*S. pombe*), Ify-1 (*C. elegans*), and PTTG1 (*H. sapiens*), respectively. Three-dimensional protein simulation was generated using the Protein Homology/Analogy Recognition Engine V 2.0 (PHYRE 2.0). Eip1 and Esp1 amino acid sequences were downloaded from the Candida Genome Database (www .candidagenome.org) and entered into PHYRE2.

REFERENCES

Agarwal R, Cohen-Fix O (2002). Phosphorylation of the mitotic regulator Pds1/securin by Cdc28 is required for efficient nuclear localization of Esp1/separase. Genes Dev 16, 1371–1382.

Alexandru G, Uhlmann F, Mechtler K, Poupart MA, Nasmyth K (2001). Phosphorylation of the cohesin subunit Scc1 by Polo/Cdc5 kinase regulates sister chromatid separation in yeast. Cell 105, 459–472.

Alexandru G, Zachariae W, Schleiffer A, Nasmyth K (1999). Sister chromatid separation and chromosome re-duplication are regulated by different mechanisms in response to spindle damage. EMBO J 18, 2707–2721.

Atir-Lande A, Gildor T, Kornitzer D (2005). Role for the SCFCDC4 ubiquitin ligase in *Candida albicans* morphogenesis. Mol Biol Cell 16, 2772–2785.

Bachewich C, Nantel A, Whiteway M (2005). Cell cycle arrest during S or M phase generates polarized growth via distinct signals in *Candida albicans*. Mol Microbiol 57, 942–959.

Bachewich C, Thomas D, Whiteway M (2003). Depletion of a polo-like kinase in *Candida albicans* activates cyclase-dependent hyphal-like growth. Mol Biol Cell 14, 2163–2180.

Bachmann G, Richards MW, Winter A, Beuron F, Morris E, Bayliss R (2016). A closed conformation of the *Caenorhabditis elegans* separase-securin complex. Open Biol 6, 160032.

Bai C, Ramanan N, Wang YM, Wang Y (2002). Spindle assembly checkpoint component CaMad2p is indispensable for *Candida albicans* survival and virulence in mice. Mol Microbiol 45, 31–44.

Bates S (2018). *Candida albicans* Cdc15 is essential for mitotic exit and cytokinesis. Sci Rep 8, 8899.

Baum P, Yip C, Goetsch L, Byers B (1988). A yeast gene essential for regulation of spindle pole duplication. Mol Cell Biol 8, 5386–5397.

Bensen ES, Clemente-Blanco A, Finley KR, Correa-Bordez J, Berman J (2005). The mitotic cyclins Clb2p and Clb4p affect morphogenesis in *Candida albicans*. Mol Biol Cell 16, 3387–3400.

Bensen ES, Filler SG, Berman J (2002). A forkhead transcription factor is important for true hyphal as well as yeast morphogenesis in *Candida albicans*. Eukaryot Cell 1, 787–798.

Care RS, Trevethick J, Binley KM, Sudbery PE (1999). The *MET3* promoter: a new tool for *Candida albicans* molecular genetics. Mol Microbiol 34, 792–798.

Caydasi AK, Ibrahim B, Pereira G (2010). Monitoring spindle orientation: Spindle position checkpoint in charge. Cell Div 5, 1–15.

Charles JF, Jaspersen SL, Tinker-Kulberg RL, Hwang L, Szidon A, Morgan DO (1998). The Polo-related kinase Cdc5 activates and is destroyed by the mitotic cyclin destruction machinery in *S. cerevisiae*. Curr Biol 8, 497–507.

Chestukhin A, Pfeffer C, Milligan S, DeCaprio JA, Pellman D (2003). Processing, localization, and requirement of human separase for normal anaphase progression. Proc Natl Acad Sci USA 100, 4574–4579.

Chou H, Glory A, Bachewich C (2011). Orthologues of the anaphase-promoting complex/cyclosome coactivators Cdc20p and Cdh1p are important for mitotic progression and morphogenesis in *Candida albicans*. Eukaryot Cell 10, 696–709.

Ciosk R, Zachariae W, Michaelis C, Shevchenko A, Mann M, Nasmyth K (1998). An ESP1/PDS1 complex regulates loss of sister chromatid cohesion at the metaphase to anaphase transition in yeast. Cell 93, 1067–1076.

Clemente-Blanco A, González-Novo A, Machín F, Caballero-Lima D, Aragón L, Sánchez M, de Aldana CR, Jiménez J, Correa-Bordes J (2006). The Cdc14p phosphatase affects late cell-cycle events and morphogenesis in *Candida albicans*. J Cell Sci 119, 1130–1143.

Cohen-Fix O, Koshland D (1997). The anaphase inhibitor of *Saccharomyces cerevisiae* Pds1p is a target of the DNA damage checkpoint pathway. Proc Natl Acad Sci USA 94, 14361–14366.

Cohen-Fix O, Peters JM, Kirschner MW, Koshland D (1996). Anaphase initiation in *Saccharomyces cerevisiae* is controlled by the APC-dependent degradation of the anaphase inhibtitor Psd1p. Genes Dev 10, 3081–3093.

Côte P, Hogues H, Whiteway MS (2009). Transcriptional analysis of the *Candida albicans* cell cycle. Mol Biol Cell 20, 3363–3373.

da Silva Dantas A, Lee KK, Raziunaite I, Schaefer K, Wagener J, Yadav B, Gow NA (2016). Cell biology of *Candida albicans*-host interactions. Curr Opin Microbiol 34, 111–118.

Finley KR, Berman J (2005). Microtubules in *Candida albicans* hyphae drive nuclear dynamics and connect cell cycle progression to morphogenesis. Eukaryot Cell 4, 1697–1711.

Finley KR, Bouchonville KJ, Quick A, Berman, J (2008). Dynein-dependent nuclear dynamics affect morphogenesis in *Candida albicans* by means of the Bub2p spindle checkpoint. J Cell Sci 121, 466–476.

Funabiki H, Kumada K, Yanagida M (1996). Fission yeast Cut1 and Cut2 are essential for sister chromatid separation, concentrate along the metaphase spindle and form large complexes. EMBO J 15, 6617–6628.

Gladfelter A, Berman J (2009). Dancing genomes: fungal nuclear positioning. Nat Rev Microbiol 7, 875–886.

Gola S, Martin R, Walther A, Dunkler A, Wendland J (2003). New modules for PCR-based gene targeting in *Candida albicans*: rapid and efficient gene targeting using 100 bp of flanking homology region. Yeast 20, 1339–1347.

González-Novo A, Labrador L, Pablo-Hernando ME, Correa-Bordes J, Sánchez M, Jiménez J, De Aldana CR (2009). Dbf2 is essential for cytokinesis and correct mitotic spindle formation in *Candida albicans*. Mol Microbiol 72, 1364–1378.

Guacci V, Yamamoto A, Strunnikov A, Kingsbury J, Hogan E, Meluh P, Koshland D (1993). Structure and function of chromosomes in mitosis of budding yeast. Cold Spring Harb Symp Quant Biol 58, 677–685.

Hatano Y, Naoki K, Suzuki A, Ushimaru T (2016). Positive feedback promotes mitotic exit via the APC/C-Cdh1-separase-Cdc14 axis in budding yeast. Cell Signal 28,1545–1554.

Hauf S, Roitinger E, Koch B, Dittrich CM, Mechtler K, Peters JM (2005). Dissociation of cohesin from chromosome arms and loss of arm cohesion during early mitosis depends on phosphorylation of SA2. PLoS Biol 3, 419–432.

Havens KA, Gardner MK, Kamieniecki RJ, Dresser ME, Dawson DS (2010). Slk19p of *Saccharomyces cerevisiae* regulates anaphase spindle dynamics through two independent mechanisms. Genetics 186, 1247–1260.

Hazan I, Sepulveda-Becerra M, Liu H (2002). Hyphal elongation is regulated independently of cell cycle in *Candida albicans*. Mol Biol Cell 13, 134–145.

Hellmuth S, Pöhlmann C, Brown A, Böttger F, Sprinzl M, Stemmann O (2015). Positive and negative regulation of vertebrate separase by Cdk1-cyclin B1 may explain why securin is dispensable. J Biol Chem 290, 8002–8010.

Hilioti Z, Chung YS, Mochizuki Y, Hardy CF, Cohen-Fix O (2001). The anaphase inhibitor Pds1 binds to the APC/C-associated protein Cdc20 in a destruction box-dependent manner. Curr Biol 11, 1347–1352.

Holt LJ, Krutchinsky AN, Morgan DO (2008). Positive feedback sharpens the anaphase switch. Nature 454, 353–357.

Hornig NCD, Knowles PP, McDonald NQ, Uhlmann F (2002). The dual mechanism of separase regulation by securin. Curr Biol 12, 973–982.

Hotz M, Lengefeld J, Barral Y (2012). The MEN mediates the effects of the spindle assembly checkpoint on Kar9-dependent spindle pole body inheritance in budding yeast. Cell Cycle 11, 3109–3116.

Jäger H, Herzig A, Lehner CF, Heidmann S (2001). *Drosophila* Separase is required for sister chromatid separation and binds to PIM and THR. Genes Dev 15, 2572–2584.

Jensen S, Segal M, Clarke DJ, Reed SI (2001). A novel role of the budding yeast separin Esp1 in anaphase spindle elongation: evidence that proper spindle association of Esp1p is regulated by Pds1. J Cell Biol 152, 27–40.

Jorgensen P, Tyers M (2004). How cells coordinate growth and division. Curr Biol 14, R1014–R1027.

Kaneva I, Sudbery I, Dickman M, Sudbery P. (2019). Proteins that physically interact with the phosphatase Cdc14 in *Candida albicans* have diverse roles in the cell cycle. Sci Rep 9, 6258.

Kitagawa R, Law E, Tang L, Rose AM (2002). The Cdc20 homolog, FZY-1, and its interacting protein, IFY-1, are required for proper chromosome segregation in *Caenorhabditis elegans*. Curr Biol 12, 2118–2123.

Kramer ER, Scheuringer N, Podtelejnikov AV, Mann M, Peters JM (2000). Mitotic regulation of the APC activator proteins CDC20 and CDH1. Mol Biol Cell 11, 1555–1569.

Kumar R (2017). Separase: function beyond cohesion cleavage and an emerging oncogene. J Cell Biochem 118, 1283–1299.

Larkin MA, Blackshields G, Brown NP, Chenna R, McGettigan PA, McWilliam H, Valentin F, Wallace IM, Wilm A, Lopez R, *et al.* (2007). Clustal W and Clustal X version 2.0. Bioinformatics 23, 2947–2948.

Lavoie H, Sellam A, Askew C, Nantel A, Whiteway M (2008). A toolbox for epitope-tagging and genome-wide location analysis in *Candida albicans*. BMC Genomics 9, 578.

Liang F, Richmond D, Wang Y (2013). Coordination of chromatid separation and spindle elongation by antagonistic activities of mitotic and S-phase CDKs. PLoS Genet 9, e1003319.

Lianga N, Doré C, Kennedy EK, Yeh E, Williams EC (2018). Cdk1 phosphorylation of Esp1/Separase functions with PP2A and Slk19 to regulate pericentric cohesin and anaphase onset. PLoS Genet 14, 1–34.

Lim HH, Goh PY, Surana U (1998). Cdc20 is essential for the cyclosome-mediated proteolysis of both Pds1 and Clb2 during M phase in budding yeast. Curr Biol 8, 231–234.

Liu HL, Osmani AH, Ukil L, Son S, Markossian S, Shen KF, Govindaraghavan M, Varadaraj A, Hashmi SB, De Souza CP, Osmani SA (2010). Single-step affinity purification for fungal proteomics. Eukaryot Cell 9, 831–833.

Lu Y, Cross F (2009). Mitotic exit in the absence of separase activity. Mol Biol Cell 20, 1576–1591.

Lundblad V, Szostak JW (1989). A mutant with a defect in telomere elongation leads to senescence in yeast. Cell 4, 633–643.

Luo S, Tong L (2018). Structural biology of the separase-securin complex with crucial roles in chromosome segregation. Curr Opin Struct Biol 49, 114–122.

McGrew JT, Goetsch L, Byers B, Baum P (1992). Requirement for ESP1 in the nuclear division of *Saccharomyces cerevisiae*. Mol Biol Cell 3, 1443–1445.

Mehta GD, Kumar R, Srivastava S, Ghosh SK (2013). Cohesin: functions beyond sister chromatid cohesion. FEBS Lett 587, 2299–2312.

Mendelsohn S, Pinsky M, Weissman Z, Kornitzer D (2017). Regulation of Candida albicans hyphal-inducing transcription factor Ume6 by the CDK1 cyclins Cln3 and Hgc1. MSphere 2, e00248-16.

Miller RK, Rose MD (1998). Kar9p is a novel cortical protein required for cytoplasmic microtubule orientation in yeast. J Cell Biol 140, 377–390.

Milne SW, Cheetham J, Lloyd D, Shaw S, Moore K, Paszkiewicz KH, Aves SJ, Bates S (2014). Role of *Candida albicans* Tem1 in mitotic exit and cytokinesis. Fungal Genet Biol 69, 84–95.

Moreno-Mateos MA, Espina ÁG, Torres B, Gámez del Estal MM, Romero-Franco A, Ríos RM, Pintor-Toro JA (2011). PTTG1/securin modulates microtubule nucleation and cell migration. Mol Biol Cell 22, 4302–4311.

Moschou P, Bozhkov PV (2012). Separases: biochemistry and function. Physiol Plant 145, 67–76.

Ofir A, Hofmann K, Weindling E, Gildor T, Barker KS, Rogers PD, Kornitzer D (2012). Role of a *Candida albicans* Nrm1/Whi5 homologue in cell cycle gene expression and DNA replication stress response. Mol Microbiol 84, 778–794.

Ofir A, Kornitzer D (2010). *Candida albicans* cyclin Clb4 carries S-phase cyclin activity. Eukaryot Cell 9, 1311–1319.

O'Meara TR, Veri AO, Ketela T, Jiang B, Roemer T, Cowen LE (2015). Global analysis of fungal morphology exposes mechanisms of host cell escape. Nat Commun 6, 1–10.

Orellana-Muñoz S, Dueñas-Santero E, Arnáiz-Pita Y, Del Rey F, Correa-Bordes J, Vázquez de Aldana CR (2018). The anillin-related Int1 protein and the Sep7 septin collaborate to maintain cellular ploidy in *Candida albicans*. Sci Rep 8, 2257.

Palou R, Palou G, Quintana DG (2017). A role for the spindle assembly checkpoint in the DNA damage response. Curr Genet 63, 275–280.

Palou G, Palou R, Zeng F, Vashisht AA, Wohlschlegel JA, Quintana DG (2015). Three different pathways prevent chromosome segregation in the presence of DNA damage or replication stress in budding yeast. PLoS Genet 11, 1–22.

Piskadlo E, Oliveira RA (2017). A topology-centric view on mitotic chromosome architecture. Int J Mol Sci 18, 2751.

Queralt E, Uhlmann F (2008). Cdk-counteracting phosphatases unlock mitotic exit. Curr Opin Cell Biol 20, 661–668.

Rahal R, Amon A (2008). The Polo-like kinase Cdc5 interacts with FEAR network components and Cdc14. Cell Cycle 7, 3262–3272.

Ramos-Morales F, Dominguez A, Romero F, Luna R, Multon MC, Pintor Toro JA, Tortolero M (2000). Cell cycle regulated expression and phosphorylation of hPTTG proto-oncogene product. Oncogene 19, 403–409.

Raspelli E, Cassani C, Chiroli E, Fraschini R (2015). Budding Yeast Swe1 is involved in the control of mitotic spindle elongation and is regulated by Cdc14 phosphatase during mitosis. J Biol Chem 290, 1–12.

Rigaut G, Shevchenko A, Rutz B, Wilm M, Mann M, Séraphin B (1999). A generic protein purification method for protein complex characterization and proteome exploration. Nat Biotechnol 17, 1030–1032.

Robert X, Gouet P (2014). Deciphering key features in protein structures with the new ENDscript server. Nucleic Acids Res W320–W324.

Rose MD, Winston F, Hieter P (1990). Methods in Yeast Genetics: A Laboratory Course Manual, New York: Cold Spring Harbor Laboratory Press.

Sanchez Y, Bachant J, Wang H, Hu F, Liu D, Tetzlaff M, Elledge SJ (1999). Control of the DNA damage checkpoint by chk1 and rad53 protein kinases through distinct mechanisms. Science 286, 1166–1171.

Sellam A, Whiteway M (2016). Recent advances on *Candida albicans* biology and virulence. F1000Res 5, 2582.

Selmecki A, Forche A, Berman, J (2010). Genomic plasticity of the human fungal pathogen *Candida albicans*. Eukaryot Cell 9, 991–1008.

Sherwood RK, Bennett RJ (2008). Microtubule motor protein Kar3 is required for normal mitotic division and morphogenesis in *Candida albicans*. Eukaryot Cell 7, 1460–1474.

Shi QM, Wang YM, Zheng XD, Lee RT, Wang Y (2007). Critical role of DNA checkpoints in mediating genotoxic-stress-induced filamentous growth in *Candida albicans*. Mol Biol Cell 18, 815–826.

Stegmeier F, Visintin R, Amon A (2002). Separase, polo kinase, the kinetochore protein Slk19, and Spo12 function in a network that controls Cdc14 localization during early anaphase. Cell 108, 207–220.

Stratmann R, Lehner CF (1996). Separation of sister chromatids in mitosis requires the *Drosophila* pimples product, a protein degraded after the metaphase/anaphase transition. Cell 84, 25–35.

Sullivan M, Uhlmann F (2003). A non-proteolytic function of separase links the onset of anaphase to mitotic exit. Nat Cell Biol 5, 249–254.

Tinker-Kulberg RL, Morgan DO (1999). Pds1 and Esp1 control both anaphase and mitotic exit in normal cells and after DNA damage. Genes Dev 13, 1936–1949.

Uhlmann F, Wernic D, Poupart MA, Koonin EV, Nasmyth K (2000). Cleavage of cohesin by the CD clan protease separin triggers anaphase in yeast. Cell 103, 375–386.

Visintin, R, Prinz, S, Amon A. (1997). CDC20 and CDH1: a family of substrate-specific activators of APC-dependent proteolysis. Science 278, 460–463.

Wang H, Gao J, Li W, Wong AHH, Hu K, Chen K, Wang Y, Sang J (2012). Pph3 Dephosphorylation of Rad53 is required for cell recovery from MMS-induced DNA damage in *Candida albicans*. PLoS One 7, 1–13.

Wang H, Liu D, Wang Y, Qin J, Elledge SJ (2001). Pds1 phosphorylation in response to DNA damage is essential for its DNA damage checkpoint function. Genes Dev 15, 1361–1372.

Weiss E (2012). Mitotic exit and separation of mother and daughter cells. Genetics 192, 1165–1202.

Woodruff JB, Drubin DG, Barnes G (2010). Mitotic spindle disassembly occurs via distinct subprocesses driven by the anaphase-promoting complex, Aurora B kinase, and kinesin-8. J Cell Biol 191, 795–808.

Yamamoto A, Guacci V, Koshland D (1996a). Pds1p is required for faithful execution of anaphase in the yeast *Saccharomyces cerevisiae*. J Cell Biol 133, 85–97.

Yamamoto A, Guacci V, Koshland D (1996b). Pds1p, an inhibitor of anaphase in budding yeast, plays a critical role in the APC and checkpoint pathway(s). J Cell Biol 133, 99–110.

Yellman CM, Roeder GS (2015). Cdc14 early anaphase release, FEAR, is limited to the nucleus and dispensable for efficient mitotic exit. PLoS One 10, e0128604.

Zou H, McGarry TJ, Bernal T, Kirschner MW (1999). Identification of a vertebrate sister-chromatid separation inhibitor involved in transformation and tumorigenesis. Science 285, 418–422.